Supplementary Information

Cognitive anchoring by large language models accelerates group consensus

Jiapeng Yang[1] Zuhua Jiang[1,*]

[1]School of Mechanical Engineering, Shanghai Jiao Tong University, Shanghai, China

[*]Correspondence: zhjiang_sjtu@126.com

Contents

1 Supplementary Methods

This Supplementary Information provides implementation details required for the Methods and Results reported in the main text. To keep the main text concise, task parameters, scoring functions, event markers, the LLM condition and model version, fNIRS preprocessing, hyperbrain graph construction, dynamic state models, statistical models and surrogate controls are documented here. Each subsection corresponds to a method or result claim in the main text and expands implementation details rather than repeating the main-text narrative. All analyses were organised using de-identified team, role, round and epoch identifiers. Supplementary Methods Table M1 maps the main-text components to the corresponding Supplementary Information sections. Supplementary Tables 1–4 summarise the behavioural, inferential, neural-fingerprint and robustness results. Appendices A–C provide de-identified English translations of the recruitment, informed-consent and ethics-approval documents; Appendices D–E provide scoring and fNIRS-coordinate reference materials.

Supplementary Methods Table M1. Main-text and Supplementary Information correspondence.

Main-text component	Supplementary location	Purpose of supplementary expansion
Participants and ethics	Sections 1.1; Appendices A–C	Recruitment criteria, consent, ethics approval and de-identified participant documents.
Task, conditions and procedure	Sections 1.2–1.7; Appendix D	Role structure, expert benchmark solution, scoring function, interface logic, LLM model version and event markers.
Behavioural acquisition and preprocessing	Section 1.8	Raw fields, team-level harmonisation, early termination handling and convergence-score construction.
fNIRS acquisition and preprocessing	Sections 1.9–1.11	Hardware, preprocessing formulae and epoch extraction rules.
Hyperbrain modelling and dynamic states	Sections 1.12–1.16; Appendix E	ROI mapping, connectivity definitions, graph metrics, WTC and HMM implementation.
Statistical analysis and robustness	Sections 1.17–1.19; Supplementary Tables 1–4	Mixed models, effect sizes, mediation, surrogate controls and numerical summaries.

1.1 Participants, recruitment and ethics

The analysed sample included 96 participants, organised into 32 three-person teams and assigned to four experimental conditions; each condition contained eight teams. Participants had a mean age of 24.3 $\pm$ 2.1 years. The gender distribution was 50 male participants and 46 female participants, corresponding to 52.08% male and 47.92% female. Participants were recruited through questionnaire

screening and targeted recruitment from populations with training and practical experience in ship structural engineering, design aesthetics, environmental engineering or closely related courses.

Inclusion criteria were age 18–35 years, ability to communicate in Mandarin, right-handedness, right-eye dominance, normal or corrected-to-normal vision, and ability to wear an fNIRS cap throughout the experiment. Main exclusion criteria were scalp inflammation or recent injury, hairstyles or headwear that substantially impeded probe contact, sensitivity to strong light or screen flicker, a history of epilepsy, self-reported use of strong sedative or stimulant medication, hierarchical or intimate relationships with another participant in the same session, and previous participation in the formal experiment or pilot experiment. Participants received monetary compensation after completing the task; withdrawals were compensated according to the completed portion. The study was approved by the Science and Technology Research Ethics Committee for Human Participants of Shanghai Jiao Tong University (approval number I20250750I), and written informed consent was obtained from all participants before data acquisition. English translations of the recruitment materials, informed-consent form and ethics-approval document are provided in Supplementary Appendices A–C.

1.2 Role structure and collaborative task

Each team comprised three participants assigned to complementary perspectives: structure/safety and performance (S), aesthetics/spatial experience (A), and environment/energy consumption (E). Role assignment was based on course training, project experience and disciplinary background reported during recruitment screening, so that every team included members who could reason from different design constraints. Role labels were kept consistent in task instructions, speaking order, behavioural records and subsequent inter-brain pair analyses.

This role structure was not intended to evaluate the individual performance of the three members separately. Instead, it constructed a group decision problem that required integration across multiple constraints. The structural role focused mainly on materials, span, partitions, fire rating and weight. The aesthetic role focused mainly on finishes, visual richness, spatial openness, window amount, beam presentation, acoustics and lighting experience. The environmental role focused mainly on air-conditioning system, recycled-material content, water fixtures, insulation package and energy-related trade-offs. Because most parameters affected multiple domains at the same time, the local optimum of one role often impaired other dimensions. For example, increasing spatial openness could improve experience while increasing structural and energy burdens; increasing fire protection and insulation could improve safety and environmental performance while increasing cost or weight. High-scoring solutions therefore required discussion to form a shared cross-role problem representation.

The collaborative task was implemented through a condition-specific browser graphical interface. In each round, the three members discussed the same set of luxury cruise-ship cabin parameters, jointly selected a complete solution and submitted it as a team. Task outcomes were recorded at the team level rather than as individual solutions. Behavioural scores therefore reflected the

quality of the team's consensus solution. The task had a single expert benchmark solution. The benchmark solution and scoring rules were calibrated using an expert engineer solution and drew on design principles for ship cabin structure, interior spatial quality, environmental engineering and safety constraints from *Ship aesthetics and cabin design* [2] and *Research and design of ship cabin environmental engineering* [3]. The score was not a post hoc subjective rating but a deterministic objective function fixed before the experiment.

1.3 Expert benchmark solution

The expert benchmark solution was hidden within the task and defined the target direction for "high-quality consensus". Participants did not see this solution during the experiment. The solution balanced structural safety, spatial experience and environmental performance while satisfying cost, weight, fire-rating and recycled-material constraints. The benchmark solution and its calculated values are listed in Supplementary Methods Table M2; finer cost/weight mappings and itemised score contributions are provided in Supplementary Appendix D.

Supplementary Methods Table M2. Expert reference solution used as the hidden task benchmark.

Code	Parameter	Value	Meaning in the benchmark solution
S1	Main frame material	0.90	Fibre-reinforced composite
S2	Column-grid density/span	0.00	Compact-column endpoint
S3	Deck and partition thickness	0.30	Single-layer integrated panel
A1	Finish and material	0.30	Industrial coating
A2	Visual richness	0.01	Near the geometric-minimal endpoint
A3	Spatial openness	0.55	Moderate openness
E1	Air-conditioning system	0.60	Heat-recovery system
E2	Recycled-material content	0.60	Mixed recycled material
E3	Water fixtures	0.90	Touchless water outlet
SA1	Window type and amount	0.00	Porthole-series endpoint
SA2	Beam presentation	0.30	Hidden integration
SE1	Envelope insulation package	0.60	Double-layer insulation
SE2	Fire rating	0.90	Enhanced zoning
AE1	Acoustic absorption scheme	0.60	Zoned absorption
AE2	Lighting (CRI/colour temperature)	0.30	Cool-white LED

In the formal scoring function, this benchmark solution had cost 704.0 and weight 313.2; therefore the cost constraint (≤ 704), weight constraint (≤ 355), fire-rating constraint (SE2 ≥ 0.9) and recycled-material constraint (E2 ≥ 0.6) were all satisfied. None of the six second-order conflict penalties was triggered, so $P_1 = \cdots = P_6 = 0$. The corresponding domain scores were structure $S = 90.35$, aesthetics $A = 63.93$ and environment $E = 80.25$. The total score was

$$T = \frac{90.35 + 63.93 + 80.25}{3} = 78.18. \tag{1}$$

Equation 1 was the expert benchmark target under the specified constraints, discrete parameter levels and 0.01 slider precision, and was not visible to participants.

1.4 Design parameters, constraints and scoring mechanism

The design interface contained 15 adjustable parameters covering structural, aesthetic, environmental and cross-domain coupling items. Discrete parameters were represented by three levels, C/B/A, from low to high or from basic to enhanced. Continuous parameters were represented by sliders indicating a continuous trade-off between two design endpoints. The complete parameter list is given in Supplementary Methods Table M3.

Supplementary Methods Table M3. Design parameters and value meanings shown in the task interface.

Code	Parameter	Value meaning
S1	Main frame material	Hot-rolled steel, quenched-and-tempered alloy steel, fibre-reinforced composite
S2	Column-grid density/span	Continuous adjustment from compact column grid to free large span
S3	Deck and partition thickness	Single-layer integrated panel, double-layer hollow construction, multi-layer damping composite
A1	Finish and material	Industrial coating, natural wood veneer, marble surface
A2	Visual richness	Continuous adjustment from geometric minimalism to refined details
A3	Spatial openness	Continuous adjustment from cellular enclosure to unbounded flow
E1	Air-conditioning system	Constant air volume, heat recovery, demand-driven system
E2	Recycled-material content	Virgin substrate, mixed recycled material, high-circularity component
E3	Water fixtures	Constant-flow faucet, flow-limiting cartridge, touchless outlet
SA1	Window type and amount	Continuous adjustment from porthole series to panoramic full-height glazing
SA2	Beam presentation	Hidden integration, skin wrapping, exposed beam styling
SE1	Envelope insulation package	Basic insulation, double-layer insulation, continuous air-tightness
SE2	Fire rating	Flame-retardant coating, fire-resistant integration, enhanced zoning
AE1	Acoustic absorption scheme	Hard reflection, zoned absorption, enveloping absorption
AE2	Lighting (CRI/colour temperature)	Cool-white LED, warm natural lighting, focused scenes

All conditions used the same task parameters, cost/weight mappings, sub-score weights and penalty rules. The interface treated cost not exceeding 704, weight not exceeding 355, high fire rating (SE2 ≥ 0.9) and at least medium recycled-material content (E2 ≥ 0.6) as core compliance constraints. The submit button was not blocked by violations, so that group search trajectories were retained; however, cost and weight violations entered the total-score penalty, and constraint status was displayed to participants at different levels of detail depending on condition.

1.5 Complete scoring formula

Let the complete solution vector be

$$\mathbf{p} = (p_{S1}, p_{S2}, p_{S3}, p_{A1}, p_{A2}, p_{A3}, p_{E1}, p_{E2}, p_{E3}, p_{SA1}, p_{SA2}, p_{SE1}, p_{SE2}, p_{AE1}, p_{AE2}). \tag{2}$$

Discrete parameters take values in $\{0.3, 0.6, 0.9\}$. Continuous slider parameters $p_{S2}, p_{A2}, p_{A3}, p_{SA1}$ take values in $[0, 1]$, with an interface step of 0.01. Cost and weight are defined as

$$C(\mathbf{p}) = \sum_i c_i(p_i), \qquad W(\mathbf{p}) = \sum_i w_i(p_i), \tag{3}$$

where item-wise mappings $c_i(\cdot)$ and $w_i(\cdot)$ are given in Supplementary Appendix D. The hard-constraint set is

$$C(\mathbf{p}) \le 704, \qquad W(\mathbf{p}) \le 355, \qquad p_{SE2} \ge 0.9, \qquad p_{E2} \ge 0.6. \tag{4}$$

Equations 2–4 define the design vector, cost–weight bookkeeping and hard compliance constraints used by all conditions.

The scoring system first computes three unpenalised base scores. The structural base score is

$$\begin{aligned} B_S = {} & 18p_{S1} + 14(1 - p_{S2}) + 16p_{S3} + 8(1 - p_{A1}) + 5(1 - p_{A2}) + 8(1 - p_{A3}) \\ & + 4(1 - p_{E1}) + f_S(p_{E2}) + 8(1 - p_{SA1}) + 8(1 - p_{SA2}) + 11p_{SE1} + 12p_{SE2} + 4(1 - p_{AE1}), \end{aligned} \tag{5}$$

where

$$f_S(p_{E2}) = \begin{cases} 7, & p_{E2} = 0.6, \\ 5, & p_{E2} = 0.3, \\ 3, & p_{E2} = 0.9. \end{cases} \tag{6}$$

The aesthetic base score is

$$\begin{aligned} B_A = {} & 12p_{S1} + 14p_{S2} + 10(1 - p_{S3}) + 20p_{A1} + 13p_{A2} + 14p_{A3} + 9p_{E1} + 9(1 - p_{E2}) \\ & + f_A(p_{E3}) + 13p_{SA1} + 11p_{SA2} + 7(1 - p_{SE1}) + 9(1 - p_{SE2}) + 11p_{AE1} + 9p_{AE2}, \end{aligned} \tag{7}$$

where

$$f_A(p_{E3}) = \begin{cases} 7, & p_{E3} = 0.9, \\ 4, & p_{E3} = 0.3, \\ 2, & p_{E3} = 0.6. \end{cases} \tag{8}$$

The environmental base score is

$$\begin{aligned} B_E = {} & 10(1 - p_{S1}) + 6(1 - p_{S2}) + 6(1 - p_{S3}) + 10(1 - p_{A1}) + 5(1 - p_{A2}) + 8(1 - p_{A3}) \\ & + 12p_{E1} + 14p_{E2} + 8p_{E3} + 8(1 - p_{SA1}) + 5(1 - p_{SA2}) \\ & + 10p_{SE1} + 6p_{SE2} + 6p_{AE1} + 6(1 - p_{AE2}). \end{aligned} \tag{9}$$

Six second-order conflict penalties are then computed:

$$P_1 = \mathbb{I}(p_{SA1} \geq 0.8,\ p_{SE1} \leq 0.3)\, 35[p_{SA1}(1 - p_{SE1})]^2, \tag{10}$$

$$P_2 = \mathbb{I}(p_{A3} \geq 0.8,\ p_{S2} \geq 0.7)\, 35[p_{A3}(1 - p_{S2})]^2, \tag{11}$$

$$P_3 = \mathbb{I}(p_{AE2} \geq 0.8,\ p_{E1} \leq 0.3)\, 30 p_{AE2}(1 - p_{E1}), \tag{12}$$

$$P_4 = \mathbb{I}(p_{A1} \geq 0.8,\ p_{E2} \leq 0.3)\, 30 p_{A1}(1 - p_{E2}), \tag{13}$$

$$P_5 = \mathbb{I}(p_{A3} \geq 0.8,\ p_{AE1} \leq 0.3)\, 38 p_{A3}(1 - p_{AE1}), \tag{14}$$

$$P_6 = \mathbb{I}(p_{S2} \geq 0.7,\ p_{S3} \leq 0.3)\, 28 p_{S2}(1 - p_{S3}). \tag{15}$$

These penalties correspond to six engineering trade-offs: large window area with low insulation, extreme openness with large span, high scene lighting with low-efficiency air conditioning, high-luxury finishes with low recycled-material content, extreme openness with low acoustic absorption, and large span with thin partitions.

Domain scores are clipped to the 0–100 range:

$$S = \mathrm{clip}_{0,100}\left(B_S - P_2 - P_6\right), \tag{16}$$

$$A = \mathrm{clip}_{0,100}\left(B_A - P_5\right), \tag{17}$$

$$E = \mathrm{clip}_{0,100}\left(B_E - P_1 - P_3 - P_4 - P_5\right), \tag{18}$$

where $\mathrm{clip}_{0,100}(x) = \min[100, \max(0, x)]$. The total score is the average of the three domain scores, with fixed soft penalties for cost and weight overruns:

$$T = \mathrm{clip}_{0,100}\left[\frac{S + A + E}{3} - 0.5\max(0, C(\mathbf{p}) - 704) - 0.5\max(0, W(\mathbf{p}) - 355)\right]. \tag{19}$$

Equations 5–19 specify the complete scoring rule. Thus, high-scoring solutions must satisfy engineering constraints and balance all three objectives; an extreme optimisation of a single dimension cannot by itself yield a high score. Participants knew that the task goal was to improve overall solution quality, but they did not know the complete scoring function or the expert benchmark solution.

1.6 Condition-specific interface logic and LLM model version

The four conditions shared identical task instructions, role assignment, parameter controls, submit button, data-saving logic and fNIRS event-triggering procedure. The experimental manipulation changed only the representation of external feedback available to the team in each round.

- **G0, no feedback.** Participants interacted only with the design-parameter interface and task instructions. The system recorded each submission's parameters, constraint status and score in the background, but did not present round-wise numeric or explanatory feedback to participants.

- **G1, numeric status feedback.** After submission, participants saw the total score and core

constraint status, such as whether cost or weight exceeded the limit, but not the sources of conflict penalties.

- **G2, rule-based explanatory feedback.** After submission, participants saw the total score, constraint status, triggered conflict penalties and trade-off advice generated from fixed rules.

- **G3, LLM prescriptive feedback.** During the predefined 2-min consultation window before submission, participants could use an interactive LLM consultation panel to ask questions about the current solution and receive prescriptive advice on parameter adjustment. After submission, the same underlying scoring function still recorded the score and constraint status. The LLM changed only the external cognitive support available to the team, not the task goal, scoring function or data-recording rules.

The manipulation therefore kept the underlying design problem identical across conditions while isolating the representational level of external feedback, from invisible to numeric, rule-based explanatory and LLM prescriptive.

The G3 consultation system used Qwen3-Max, model version `qwen3-max-2025-09-23`, as the language model for the AI consultation condition. The implementation called the DashScope OpenAI-compatible chat-completions endpoint with the model field `qwen3-max` and temperature set to 0.5.

The consultation interface used a fixed system prompt that instructed the model to act as a senior luxury cruise-cabin design consultant for a team consisting of structural, aesthetic and environmental roles. The prompt encoded task-domain reference information derived from the cabin-design textbook references, including parameter meanings, core hard constraints, three-objective score logic and hidden trade-off penalty rules. The per-query user prompt supplied the current solution state: total and domain scores, cost, weight, hard-constraint status, current parameter values as JSON and the team's natural-language question. The prompt did not include the expert benchmark solution, complete scoring formula, neural data, participant identity, other teams' information or post hoc analysis results.

The consultation panel retained the user–AI dialogue in the on-screen session log, giving the team a visible within-session memory of earlier questions and advice during consultation. This consultation memory was separate from the hidden benchmark solution and did not allow the model to access information outside the current team's interface state. The model output was displayed as design suggestions rather than as an automatic parameter update; the team still had to discuss and submit its own solution. The system could not change the deterministic scoring function, directly submit a solution, observe neural data or access information about other teams.

1.7 Temporal structure, event markers and early termination

The experiment contained up to five nominal decision rounds. Before iterative design, all teams completed a 30-s resting baseline and 5 min of task-material reading. Each nominal round contained an 8.5-min rest/sequential-discussion window and a 2-min team-decision window; the 8.5-min window

consisted of 30 s of rest and up to 8 min of sequential discussion. G1, G2 and G3 also had a 1-min feedback and reflection-recording window after each round submission, whereas G0 presented no feedback. After all nominal rounds, teams completed a 1-min final solution confirmation and an approximately 2-min questionnaire.

Sequential discussion was used to control speaking opportunity and role-exposure order. In each round, participants spoke in the fixed order structure (S) → aesthetics (A) → environment (E). While one member was speaking, the other members did not interrupt, evaluate or guide by hints. A single speaking turn was limited to approximately 90 s; if there was no additional point, the speaker could briefly pass. One speaking cycle consisted of one turn by each of the three members, and the discussion window ended when time expired and proceeded to group decision. In G3, the sequential-discussion window was further divided into pre-consultation discussion, 2 min of LLM consultation and post-consultation discussion, allowing AI consultation to be embedded without changing the overall within-round structure.

Event-marker structure differed by condition.

G0–G2 event structure. Only three event types were used: mark 1 = rest start, mark 2 = rest end, and mark 3 = round submission. These conditions contained 17 markers in total, with the sequence

$$1\text{-}2\text{-}1\text{-}2\text{-}3\text{-}1\text{-}2\text{-}3\text{-}1\text{-}2\text{-}3\text{-}1\text{-}2\text{-}3\text{-}1\text{-}2\text{-}3. \tag{20}$$

The marker sequence in Eq. 20 was used for G0–G2. The first mark1–mark2 interval corresponded to the pre-task baseline. Each subsequent round contained one rest epoch and one sequential-discussion/decision epoch. Rounds 1–4 also contained an inter-round interval, which served as a transition interval in G0 and as a feedback-and-recording epoch in G1 and G2.

G3 event structure. Five event types were used: mark 1 = rest start, mark 2 = rest end, mark 3 = round submission, mark 4 = AI consultation start and mark 5 = AI consultation end. The typical within-round sequence was

$$1\text{-}2\text{-}4\text{-}5\text{-}3, \tag{21}$$

corresponding to rest, pre-consultation discussion, AI consultation, post-consultation discussion/team decision and submission. Equation 21 therefore defines the within-round segmentation used for G3. The first mark1–mark2 interval again corresponded to the pre-task baseline.

Early termination rule. All teams were informed in advance that they could jointly request early termination if they believed the current design was sufficiently good. Under this rule, the final accepted solution was treated as the solution for the remaining nominal rounds in the behavioural record. This behavioural carry-forward rule was used only to keep the nominal round-by-team trajectory matrix complete; neural data and epoch-duration summaries were never carried forward and were always segmented according to the actually recorded event markers.

1.8 Behavioural data acquisition and harmonisation

Behavioural data were generated automatically by the experimental interface at each round submission. Each submission record contained 15 design parameters, cost, weight, hard-constraint violation status, six conflict penalties, structural/aesthetic/environmental sub-scores, total score, validity flag and submission timestamp. All behavioural records were organised using de-identified team, role and round identifiers and contained no participant names or contact details.

During behavioural harmonisation, submitted solution parameters, constraint status, cost/weight metrics and score results were first extracted by team, role and round index and then organised into a long-format table. The harmonised fields included `group`, `triad_id`, `role`, `round`, `total_score`, `s_score`, `a_score`, `e_score`, `is_valid`, `cost`, `weight` and `is_filled`.

The primary behavioural analysis used the team total score in each round as the solution-quality metric and used structural, aesthetic and environmental sub-scores to describe the domain composition of solution quality. For the same team and round, the three role-side records were aggregated into one team-by-round observation after consistency checks. Behavioural convergence was represented by the linear slope of team total score across nominal rounds. Early termination was handled according to the predefined rule in Section 1.7; neural analyses still extracted epochs from the actual event markers.

1.9 fNIRS acquisition hardware

Cortivision Photon Cap (Model C20) and Cortivision Pathfinder software were used to record cortical haemodynamic activity simultaneously from the three members of each team. The final analysis set contained SNIRF records from 32 teams and 96 participants. Acquisition used two wavelengths, 760 and 850 nm; 26 physical channels per participant; and 52 dual-wavelength measurement-list entries per SNIRF file. Thus, each team had 78 physical channel time series, and the full sample contained $96 \times 26 = 2{,}496$ participant-by-channel time series and $96 \times 52 = 4{,}992$ dual-wavelength measurement series. Optode placement followed the extended 10–5 layout system. Empirical sampling rates varied slightly across files (5.29–5.62 Hz; mean approximately 5.50 Hz), and the exact value was read from each SNIRF header during preprocessing.

1.10 Signal preprocessing pipeline

Preprocessing was implemented in Python using MNE-NIRS. For each participant, raw light intensity $I_\lambda(t)$ was converted to optical-density change:

$$\Delta \mathrm{OD}_\lambda(t) = -\ln \frac{I_\lambda(t)}{I_{\lambda,0}}, \tag{22}$$

where $\lambda \in \{760, 850\}$ nm and $I_{\lambda,0}$ denotes baseline light intensity. Motion artifacts were corrected using temporal derivative distribution repair (TDDR), a robust derivative-based algorithm that suppresses spike-like and baseline-shift artifacts while preserving slower haemodynamic structure [1].

TDDR was applied before haemoglobin conversion.

Corrected optical density was converted to oxygenated and deoxygenated haemoglobin concentration changes using the modified Beer–Lambert law [4]:

$$\begin{pmatrix}\Delta[\mathrm{HbO}](t)\\ \Delta[\mathrm{HbR}](t)\end{pmatrix} = \frac{1}{d}\begin{pmatrix}\varepsilon^{760}_{\mathrm{HbO}}\,\mathrm{DPF}_{760} & \varepsilon^{760}_{\mathrm{HbR}}\,\mathrm{DPF}_{760}\\ \varepsilon^{850}_{\mathrm{HbO}}\,\mathrm{DPF}_{850} & \varepsilon^{850}_{\mathrm{HbR}}\,\mathrm{DPF}_{850}\end{pmatrix}^{-1}\begin{pmatrix}\Delta\mathrm{OD}'_{760}(t)\\ \Delta\mathrm{OD}'_{850}(t)\end{pmatrix}, \tag{23}$$

where d is the source–detector distance and the differential pathlength factors were fixed as $\mathrm{DPF}_{760} = \mathrm{DPF}_{850} = 6.0$. The primary analyses used HbO.

Signals were then band-pass filtered between 0.01 and 0.10 Hz using a fourth-order Butterworth filter:

$$x_c(t) = \mathrm{BPF}_{[0.01,0.10]\,\mathrm{Hz}}(\Delta[\mathrm{HbO}]_c(t)). \tag{24}$$

Equations 22–24 define the full preprocessing transformation from raw light intensity to filtered HbO signals.

1.11 Epoch extraction

In this study, an epoch denotes a task-phase time window cut from the continuous HbO time series according to event markers. It is the basic analysis unit for ROI aggregation, inter-brain connectivity estimation and dynamic state modelling. Each epoch corresponded to a clearly defined experimental phase, such as rest, discussion, feedback, AI consultation or post-consultation decision.

Continuous HbO signals were segmented using corrected event-marker files. Event markers were first extracted from SNIRF records and checked according to the condition-specific sequences described in Section 1.7. Occasional duplicate, missing or out-of-order markers were corrected using predefined sequence rules and synchronous recordings from the same team. Correction decisions were made before neural connectivity analysis and used only event-order rules and same-session synchronous team recordings, not behavioural scores or neural synchrony outcomes. Corrected markers were used to extract within-round phases for each condition: G0–G2 included rest and discussion phases, G1 and G2 also included feedback phases, and G3 included rest, pre-consultation discussion, AI consultation and post-consultation decision phases. Epoch metadata included round number, phase label, start time, end time and sample count.

1.12 ROI aggregation

This section corresponds to the main-text ROI-aggregation subsection under “Hyperbrain modelling and dynamic-state definitions” and provides implementation details for ROI-related symbols in the main-text notation table. The main text reports only the ROI aggregation principle and a summary of channel–ROI mapping. This section supplements channel localisation, functional ROI grouping rules, weight definitions and output data structures. The correspondence between the modelling components in the main text and the Supplementary Information is summarised in Supplementary Methods Table M4.

Supplementary Methods Table M4. Main-text modelling components and their Supplementary Information locations.

Main-text modelling component	Supplementary location	Supplementary content
Unified notation	Sections 1.12–1.16	Concrete meanings of derived symbols and implementation parameters in each modelling step.
ROI aggregation	Section 1.12 and Appendix E	Channel MNI coordinates, AAL3 mapping, functional ROI grouping and weighted channel aggregation.
Hyperbrain graph construction	Section 1.15	21-node hyperbrain graph, 147 inter-brain edges, block adjacency matrix, homologous/complementary edge sets and graph metrics.
Inter-brain synchrony metrics	Sections 1.13–1.15	Pearson-Fisher-z synchrony, WTC frequency-specific synchrony and summary metrics including GS, HS and CS.
Dynamic connectivity and neural fingerprints	Section 1.16	Sliding-window connectivity vectors, PCA reduction, HMM state estimation, neural-fingerprint back-projection and dynamic state metrics.

Channel coordinates were located in MNI standard space and mapped to the AAL3 atlas according to fNIRS spatial-registration methods [5, 6, 7, 8]. AAL3 labels were used for anatomical localisation, and Brodmann areas (BAs) were used to report regional attributes. The main analyses did not model single AAL3 regions directly; instead, adjacent and functionally related channels were grouped into seven functional regions of interest (ROIs): frontopolar area (FPA), dorsolateral prefrontal cortex (DLPFC), medial prefrontal cortex (mPFC), middle temporal gyrus (MTG), superior temporal gyrus (STG), primary somatosensory cortex (S1) and supramarginal gyrus (SMG). Each channel's MNI coordinates, AAL3 label and BA mapping are listed in Supplementary Appendix E. The channel sets for the seven ROIs are shown in Supplementary Methods Table M5.

Supplementary Methods Table M5. ROI channel sets used for functional aggregation.

ROI	No. channels	Channel set $\mathcal{C}_k$
FPA	8	Fpz_Fp1, Fpz_Fp2, AF3_Fp1, AF3_AFz, AF4_AFz, AF4_Fp2, F3_F1, Fz_F1
DLPFC	9	AF7_Fp1, AF8_Fp2, AF7_AFF5h, AF3_AFF5h, AF4_AFF6h, AF8_AFF6h, F3_AFF5h, F4_F2, F4_AFF6h
mPFC	2	Fpz_AFz, Fz_F2
MTG	4	FTT9h_T7, TTP7h_T7, FTT9h_FT7, FTT7h_T7
STG	1	FTT7h_FT7
S1	1	FTT7h_C5
SMG	1	TTP7h_C5

Let $x_{g,m,c,e}(t)$ denote the preprocessed HbO time series of member m in team g, physical channel c, epoch e, and let $\mathcal{C}_k$ denote the channel set mapped to ROI k. For an ROI containing multiple channels, channel time series were aggregated using amplitude-to-variability weights:

$$x_{g,m,k,e}(t) = \frac{\sum_{c\in\mathcal{C}_k} w_{g,m,c,e}\, x_{g,m,c,e}(t)}{\sum_{c\in\mathcal{C}_k} w_{g,m,c,e}}, \tag{25}$$

where

$$w_{g,m,c,e} = \frac{\overline{|x_{g,m,c,e}|}}{\sigma\left(x_{g,m,c,e}\right)}. \tag{26}$$

In Eq. 26, $\overline{|x_{g,m,c,e}|}$ denotes the mean absolute amplitude of the channel in the current epoch, and $\sigma(x_{g,m,c,e})$ denotes the channel standard deviation in that epoch. The weight determines only the relative contribution of channels within the same member, epoch and ROI, and does not enter subsequent statistical models. For single-channel ROIs, $x_{g,m,k,e}(t)$ is directly equal to the corresponding channel time series. The output of Eq. 25 is seven ROI HbO time series for each participant and each epoch, which serve as the input to all connectivity analyses in Sections 1.13–1.16.

1.13 Static inter-brain connectivity

This section corresponds to the Pearson-Fisher-z synchrony definition in the main-text inter-brain synchrony subsection and provides the basis for the hyperbrain graph edge weights in Section 1.15. Static inter-brain connectivity refers to linear temporal coupling between two members' ROI time series over a complete epoch. For team g, epoch e, member pair $(m, n) \in \mathcal{P}$ and ROI pair (i, j), Pearson correlation is defined as

$$\rho_{ij,g,e}^{(m,n)} = \frac{\sum_{t\in e}\left(x_{g,m,i,e}(t) - \bar{x}_{g,m,i,e}\right)\left(x_{g,n,j,e}(t) - \bar{x}_{g,n,j,e}\right)}{\sqrt{\sum_{t\in e}\left(x_{g,m,i,e}(t) - \bar{x}_{g,m,i,e}\right)^2}\sqrt{\sum_{t\in e}\left(x_{g,n,j,e}(t) - \bar{x}_{g,n,j,e}\right)^2}}, \tag{27}$$

where $\bar{x}_{g,m,i,e}$ is the temporal mean of ROI i for member m in epoch e. The correlation coefficient was then Fisher-z transformed:

$$Z_{ij,g,e}^{(m,n)} = \operatorname{arctanh}\left(\rho_{ij,g,e}^{(m,n)}\right) = \frac{1}{2}\ln\frac{1+\rho_{ij,g,e}^{(m,n)}}{1-\rho_{ij,g,e}^{(m,n)}}. \tag{28}$$

In implementation, zero-variance ROI series were handled by denominator protection before the Pearson calculation, and correlation coefficients were clipped to $[-0.9999, 0.9999]$ before applying Eq. 28. This kept the Fisher-z transform finite without changing the definition of the metric for ordinary non-boundary correlations.

The member-pair set was fixed as

$$\mathcal{P} = \{(A, S), (A, E), (S, E)\}. \tag{29}$$

This pair order was used consistently in stored matrices and dynamic-connectivity vectors. Thus, each team in each epoch yielded three 7×7 inter-brain connectivity matrices:

$$\boldsymbol{Z}_{g,e}^{mn} = \left[Z_{ij,g,e}^{(m,n)} \right]_{i,j=1}^{7}, \qquad (m,n) \in \mathcal{P}. \tag{30}$$

Equations 27–30 define the static Fisher-z connectivity matrices used by the hyperbrain graph. Each matrix contained 49 ROI–ROI inter-brain edges, yielding 147 inter-brain edges across the three member pairs. Edges with $i = j$ were defined as homologous edges, and edges with $i \neq j$ as complementary edges. Fisher-z edge weights retained the sign of synchrony; strength metrics such as GS, HS and CS used absolute values to measure coupling magnitude rather than positive or negative direction.

In addition to inter-brain edges, the cognitive-offloading analysis used individual DLPFC HbO amplitude as a within-brain prefrontal-load metric. For member m, DLPFC load was defined as the mean absolute HbO amplitude of the DLPFC ROI during the corresponding phase:

$$L_{g,m,e}^{\mathrm{DLPFC}} = \frac{1}{|T_e|} \sum_{t \in e} \left| x_{g,m,\mathrm{DLPFC},e}(t) \right|, \tag{31}$$

where $|T_e|$ is the number of time points in the epoch. Equation 31 is not a hyperbrain graph edge weight; it is used for the mechanistic comparison between inter-brain synchrony and within-brain load in the main-text cognitive-alignment/offloading analysis.

1.14 Wavelet transform coherence

This section corresponds to the second of the two complementary synchrony metrics in the main-text inter-brain synchrony subsection. Pearson-Fisher-z connectivity quantifies broadband temporal correlation over the whole epoch, whereas wavelet transform coherence (WTC) evaluates whether synchrony is also observable in task-related low-frequency oscillations [9]. The frequency band was predefined as 0.02–0.05 Hz, consistent with low-frequency ranges used in fNIRS analyses of social interaction and task-related haemodynamic oscillations.

The implementation used a complex Morlet continuous wavelet transform with the `cmor1.5-1.0` wavelet and scales corresponding to 0.02–0.05 Hz. For two ROI time series $x(t)$ and $y(t)$, let $W_x(s,\tau)$ and $W_y(s,\tau)$ be their wavelet transforms, where s is scale and τ is temporal position. The cross-wavelet spectrum is

$$W_{xy}(s,\tau) = W_x(s,\tau) W_y^*(s,\tau), \tag{32}$$

where * denotes complex conjugation. Squared wavelet coherence is defined as

$$R_{xy}^2(s,\tau) = \frac{\left| G_t\left(W_{xy}(s,\tau)\right) \right|^2}{G_t\left(|W_x(s,\tau)|^2\right) G_t\left(|W_y(s,\tau)|^2\right)}, \tag{33}$$

where $G_t(\cdot)$ denotes Gaussian smoothing along the temporal dimension, using a standard deviation of $\max(1, \lfloor 3 f_s \rfloor)$ samples for sampling rate f_s. Zero denominators were replaced by 1 before division.

Let $\mathcal{S}_{0.02-0.05}$ be the scale set corresponding to 0.02–0.05 Hz and let $\mathcal{T}_e$ be the retained time points in epoch e. The epoch-level WTC synchrony for member pair (m, n) and ROI pair (i, j) is

$$C_{ij,g,e}^{(m,n)} = \frac{1}{|\mathcal{T}_e|\,|\mathcal{S}_{0.02-0.05}|} \sum_{\tau \in \mathcal{T}_e} \sum_{s \in \mathcal{S}_{0.02-0.05}} R_{ij,g,e}^{2,(m,n)}(s, \tau). \tag{34}$$

Equations 32–34 define the WTC synchrony pipeline. $C_{ij,g,e}^{(m,n)}$ ranges from 0 to 1, with larger values indicating stronger coherence in the corresponding band. WTC matrices have the same member-pair and ROI-pair structure as Pearson-Fisher-z matrices; they can therefore be summarised using the same graph structure in Section 1.15 to obtain WTC versions of GS, HS and CS. Because WTC is a non-negative coherence metric, no Fisher-z transformation was applied to WTC summaries.

1.15 Hyperbrain network metrics

This section corresponds to the main-text hyperbrain graph and synchrony-metric subsections and supplements the block-matrix representation of the hyperbrain graph, homologous/complementary edge sets and graph-metric calculations. Each team in each epoch was represented as a weighted undirected hyperbrain graph:

$$\mathcal{G}_{g,e} = (\mathcal{V}_{g,e}, \mathcal{E}_{g,e}, \boldsymbol{B}_{g,e}). \tag{35}$$

The node set was the Cartesian product of members and ROIs:

$$\mathcal{V}_{g,e} = \mathcal{M} \times \mathcal{K}, \qquad \mathcal{M} = \{A, S, E\}, \quad \mathcal{K} = \{1, \ldots, 7\}, \qquad |\mathcal{V}_{g,e}| = 21. \tag{36}$$

The edge set contained only inter-brain edges between different members:

$$\mathcal{E}_{g,e} = \{((m, i), (n, j)) : (m, n) \in \mathcal{P},\, i, j \in \mathcal{K}\}, \qquad |\mathcal{E}_{g,e}| = 147. \tag{37}$$

Equations 35–37 define the 21-node, 147-edge hyperbrain graph. Within-member ROI–ROI correlations did not enter the hyperbrain graph edge set, so graph metrics reflected inter-brain synchrony only.

If nodes were ordered as $(A, 1), \ldots, (A, 7), (S, 1), \ldots, (S, 7), (E, 1), \ldots, (E, 7)$, the block adjacency matrix was

$$\boldsymbol{B}_{g,e} = \begin{pmatrix} \mathbf{0} & \boldsymbol{Z}_{g,e}^{AS} & \boldsymbol{Z}_{g,e}^{AE} \\ (\boldsymbol{Z}_{g,e}^{AS})^\top & \mathbf{0} & \boldsymbol{Z}_{g,e}^{SE} \\ (\boldsymbol{Z}_{g,e}^{AE})^\top & (\boldsymbol{Z}_{g,e}^{SE})^\top & \mathbf{0} \end{pmatrix}. \tag{38}$$

The diagonal blocks were fixed at zero because they corresponded to within-person rather than inter-brain connections. The off-diagonal blocks were formed from the Fisher-z inter-brain connectivity matrices defined in Section 1.13.

The homologous and complementary edge sets were defined as

$$\mathcal{E}^{\mathrm{H}}_{g,e} = \{((m,i),(n,i)) : (m,n) \in \mathcal{P},\, i \in \mathcal{K}\}, \qquad |\mathcal{E}^{\mathrm{H}}_{g,e}| = 21, \tag{39}$$

$$\mathcal{E}^{\mathrm{C}}_{g,e} = \{((m,i),(n,j)) : (m,n) \in \mathcal{P},\, i,j \in \mathcal{K},\, i \neq j\}, \qquad |\mathcal{E}^{\mathrm{C}}_{g,e}| = 126. \tag{40}$$

Global strength, homologous strength and complementary strength were defined as

$$\mathrm{GS}_{g,e} = \frac{1}{147} \sum_{(m,n)\in\mathcal{P}} \sum_{i=1}^{7}\sum_{j=1}^{7} \left| Z^{(m,n)}_{ij,g,e} \right|, \tag{41}$$

$$\mathrm{HS}_{g,e} = \frac{1}{21} \sum_{(m,n)\in\mathcal{P}} \sum_{i=1}^{7} \left| Z^{(m,n)}_{ii,g,e} \right|, \tag{42}$$

$$\mathrm{CS}_{g,e} = \frac{1}{126} \sum_{(m,n)\in\mathcal{P}} \sum_{i\neq j} \left| Z^{(m,n)}_{ij,g,e} \right|. \tag{43}$$

Equations 38–41 specify the matrix representation and the three global edge-category summaries used in the main text.

Pair-specific strength was used to describe the average synchrony of a particular member pair:

$$\mathrm{PS}^{(m,n)}_{g,e} = \frac{1}{49} \sum_{i=1}^{7}\sum_{j=1}^{7} \left| Z^{(m,n)}_{ij,g,e} \right|. \tag{44}$$

Node strength was used to describe the total connection strength of a particular member's ROI in the hyperbrain graph:

$$\mathrm{NS}^{(m,i)}_{g,e} = \frac{1}{14} \sum_{\substack{n\in\mathcal{M}\\ n\neq m}} \sum_{j=1}^{7} \left| \boldsymbol{B}_{g,e}[(m,i),(n,j)] \right|. \tag{45}$$

ROI-specific DLPFC inter-brain synchrony was defined as the average homologous DLPFC–DLPFC edge across the three member pairs:

$$\mathrm{IBS}^{\mathrm{DLPFC}}_{g,e} = \frac{1}{3} \sum_{(m,n)\in\mathcal{P}} \left| Z^{(m,n)}_{\mathrm{DLPFC,DLPFC},g,e} \right|. \tag{46}$$

Equations 44–46 define secondary summaries used for member-pair, node-level and DLPFC-specific analyses.

To make phase meaning comparable in cross-condition analyses, G3 pre-consultation discussion and post-consultation decision were merged into a discussion-equivalent phase. For any metric M, the merging rule was a duration-weighted average:

$$M_{\mathrm{disc.eq}} = \frac{d_{\mathrm{pre}} M_{\mathrm{pre}} + d_{\mathrm{post}} M_{\mathrm{post}}}{d_{\mathrm{pre}} + d_{\mathrm{post}}}, \tag{47}$$

where d_{pre} and d_{post} are the durations of the pre-consultation discussion and post-consultation decision phases. Equation 47 was used only to align discussion phases across conditions; within-G3

mechanistic comparisons between pre-consultation discussion and AI consultation retained the original phase labels.

1.16 Dynamic connectivity and hidden Markov modelling

This section corresponds to the main-text dynamic-connectivity and neural-fingerprint subsection and supplements the full modelling procedure for dynamic connectivity, HMM state estimation and neural fingerprints. Dynamic connectivity was defined as the temporal trajectory of hyperbrain edge weights across consecutive sliding windows. The window length was $L = 30$ s, step size was $\Delta = 3$ s and the window function was a Hann window $h(\cdot)$. For an epoch of duration d_e, the number of available windows was

$$W_e = \left\lfloor \frac{d_e - L}{\Delta} \right\rfloor + 1, \qquad d_e \geq L. \tag{48}$$

In implementation, actual timestamps were used to determine window boundaries, and second-level windows were mapped to sample points according to the sampling rate.

Within window w, ROI time series were weighted by the window function:

$$x^{(w)}_{g,m,k,e}(t) = h(t - \tau_w) x_{g,m,k,e}(t), \tag{49}$$

where τ_w is the window centre. Window-level Fisher-z inter-brain connectivity matrices $\boldsymbol{Z}^{mn}_{g,e,w}$ were then calculated using the same formulae as in Section 1.13. The connectivity matrices for the three member pairs were vectorised and concatenated in a fixed order into a 147-dimensional vector:

$$\mathbf{v}_{g,e,w} = \left[\mathrm{vec}\left(\boldsymbol{Z}^{AS}_{g,e,w}\right); \mathrm{vec}\left(\boldsymbol{Z}^{AE}_{g,e,w}\right); \mathrm{vec}\left(\boldsymbol{Z}^{SE}_{g,e,w}\right) \right] \in \mathbb{R}^{147}. \tag{50}$$

Equations 48–50 define the sliding-window observations. Here $\mathrm{vec}(\cdot)$ denotes vectorisation using a fixed ROI order. Across all available epochs, this procedure yielded $Q = 370$ continuous epoch segments and $N = 22{,}256$ windows.

To reduce instability in high-dimensional covariance estimation, window vectors were first centred at the edge level:

$$\tilde{\mathbf{v}}_\ell = \mathbf{v}_\ell - \bar{\mathbf{v}}, \qquad \ell = 1, \ldots, N, \tag{51}$$

where $\bar{\mathbf{v}}$ is the mean connectivity vector across all windows. Principal component analysis was then performed using full singular-value decomposition:

$$\mathbf{u}_\ell = \boldsymbol{P}_d^\top \tilde{\mathbf{v}}_\ell, \qquad \mathbf{u}_\ell \in \mathbb{R}^d. \tag{52}$$

Equations 51 and 52 define edge-wise centring and PCA reduction. $\boldsymbol{P}_d \in \mathbb{R}^{147 \times d}$ is the loading matrix of the first d principal components. We retained $d = 87$ components, which explained 90.1% of the variance.

The HMM represented each window's low-dimensional connectivity pattern as a Gaussian emission from a discrete latent state. For continuous segment q, let its observation sequence be

$\mathbf{U}^{(q)} = (\mathbf{u}_{q,1}, \ldots, \mathbf{u}_{q,N_q})$ and its latent state sequence be $\mathbf{s}^{(q)} = (s_{q,1}, \ldots, s_{q,N_q})$. Given state number K, the model is

$$P(s_{q,1} = k) = \pi_k, \tag{53}$$

$$P(s_{q,\ell} = b \mid s_{q,\ell-1} = a) = A_{ab}, \tag{54}$$

$$\mathbf{u}_{q,\ell} \mid s_{q,\ell} = k \sim \mathcal{N}\left(\boldsymbol{\mu}_k, \boldsymbol{\Sigma}_k\right), \tag{55}$$

where $\boldsymbol{\pi}$ is the initial state distribution, $\boldsymbol{A}$ is the state-transition matrix, and $\boldsymbol{\mu}_k$ and $\boldsymbol{\Sigma}_k$ are the mean vector and full covariance matrix of state k. The joint likelihood for one segment is

$$p\left(\mathbf{U}^{(q)}, \mathbf{s}^{(q)} \mid \theta_K\right) = \pi_{s_{q,1}} \mathcal{N}\left(\mathbf{u}_{q,1}; \boldsymbol{\mu}_{s_{q,1}}, \boldsymbol{\Sigma}_{s_{q,1}}\right) \prod_{\ell=2}^{N_q} A_{s_{q,\ell-1} s_{q,\ell}} \mathcal{N}\left(\mathbf{u}_{q,\ell}; \boldsymbol{\mu}_{s_{q,\ell}}, \boldsymbol{\Sigma}_{s_{q,\ell}}\right), \tag{56}$$

and the full-data likelihood is the product of the likelihoods of the 370 segments. Let $\mathbf{U}$ denote the collection of all segment observation sequences. Models were fitted for $K = 2, \ldots, 7$, with 10 random initialisations and 200 expectation-maximisation iterations for each candidate K. The state number was determined from the Bayesian information criterion curve and model parsimony:

$$\mathrm{BIC}(K) = -2 \ln \hat{L}(K) + n_{\mathrm{param}}(K) \ln N, \tag{57}$$

where $\hat{L}(K)$ is the maximum likelihood for the model with K states and $N = 22{,}256$ is the number of windows. The number of free parameters in a full-covariance HMM is

$$n_{\mathrm{param}}(K) = (K-1) + K(K-1) + K\left[d + \frac{d(d+1)}{2}\right], \tag{58}$$

corresponding respectively to the initial distribution, transition matrix, state means and state covariance matrices. The most likely state sequence was decoded using the Viterbi algorithm:

$$\hat{\mathbf{s}} = \arg\max_{\mathbf{s}} p\left(\mathbf{s} \mid \mathbf{U}, \hat{\theta}_K\right). \tag{59}$$

Equations 53–59 specify the HMM emission, likelihood, model selection and decoding steps. For each candidate K, the analysis used 10 seeded random initialisations, retained the maximum-likelihood fit across starts and archived the selected model outputs, including decoded state sequences, transition probabilities, state means in both PCA and original edge space, PCA loadings, fractional occupancy, mean dwell time, switching rates and model-level transition entropy. The absolute BIC was lowest at $K = 6$, but the improvement from $K = 5$ to $K = 6$ was small relative to earlier decreases and $K = 7$ rebounded; we therefore report the HMM choice as an elbow-and-parsimony selection rather than as a strict minimum-BIC rule. The numerical selection trail is summarised in Supplementary Table 3 and visualised in Supplementary Fig. 1.

We refer to recurrent state-specific connectivity patterns in the HMM as neural fingerprints. The term has a precise mathematical definition in the model: the neural fingerprint of state k is

the vector obtained by back-projecting its Gaussian emission mean in PCA space to the original 147-dimensional inter-brain connectivity space:

$$\mathbf{f}_k = \bar{\mathbf{v}} + \boldsymbol{P}_d \boldsymbol{\mu}_k, \qquad \mathbf{f}_k \in \mathbb{R}^{147}. \tag{60}$$

Each element of Eq. 60 corresponds to a fixed member-pair by ROI-pair inter-brain edge. Thus, $\mathbf{f}_k$ can be reorganised into three 7×7 member-pair connectivity matrices to interpret the hyperbrain topology of different states.

After state decoding, let $\mathcal{L}_a$ be the window-index set for any analysis unit a, such as condition, phase or triad, and let $\mathcal{T}_a = \{\ell : \ell \in \mathcal{L}_a, \ell - 1 \in \mathcal{L}_a\}$ be the set of adjacent transition indices. The fractional occupancy of state k is

$$\mathrm{FO}_{a,k} = \frac{1}{|\mathcal{L}_a|} \sum_{\ell \in \mathcal{L}_a} \mathbb{I}\left(\hat{s}_\ell = k\right). \tag{61}$$

Let $\mathcal{R}_{a,k}$ be the set of continuous dwell segments of state k in analysis unit a, and let n_r^{run} be the number of windows in dwell segment r. Mean dwell time is

$$\mathrm{MDT}_{a,k} = \Delta \cdot \frac{1}{|\mathcal{R}_{a,k}|} \sum_{r \in \mathcal{R}_{a,k}} n_r^{\mathrm{run}}. \tag{62}$$

Overall switching rate is

$$\mathrm{SR}_a = \frac{1}{|\mathcal{T}_a|} \sum_{\ell \in \mathcal{T}_a} \mathbb{I}\left(\hat{s}_\ell \neq \hat{s}_{\ell-1}\right). \tag{63}$$

The fitted transition matrix also provided a model-level transition-entropy summary:

$$\mathrm{TE}_{\mathrm{model}} = -\sum_{p=1}^{K} \sum_{q=1}^{K} A_{pq} \log_2 \left(A_{pq} + \varepsilon\right), \tag{64}$$

where ε is a small positive constant used to avoid $\log 0$. Equations 61–64 define the dynamic-state summary metrics used in the Supplementary tables and figures. FO describes state occupancy, MDT describes stable duration, SR describes switching frequency and $\mathrm{TE}_{\mathrm{model}}$ describes uncertainty in the fitted state-transition matrix. Together, these metrics characterise the dynamic organisation of neural fingerprints reported in the main text.

1.17 Statistical analysis pipeline, behavioural convergence and neural–behavioural association

This section corresponds to the statistical-analysis overview in the main text and supplements the concrete formulae for behavioural convergence and neural–behavioural association. The correspondence between main-text statistical components and the statistical parts of the Supplementary Information is shown in Supplementary Methods Table M6.

Supplementary Methods Table M6. Main-text statistical components and their Supplementary Information locations.

Main-text statistical component	Supplementary location	Supplementary content
Analysis units and overall principles	Section 1.17	Triad as primary inference unit, round/epoch as repeated observation, two-sided tests and FDR principles.
Behavioural trajectory and convergence speed	Section 1.17	Team-by-round behavioural table, convergence slope, final performance and dispersion.
Static hyperbrain synchrony	Section 1.18	Linear mixed-effects models for Pearson GS and WTC GS, duration covariate, non-parametric robustness tests and effect sizes.
Homologous/complementary connection categories	Section 1.18	Condition × connection-type mixed model.
Dynamic neural-fingerprint summaries	Sections 1.16 and 1.18	HMM modelling, state metrics, condition/phase-level fractional occupancy and model-level transition summaries.
Cognitive-alignment and cognitive-offloading mechanism test	Section 1.18	Within-G3 pre-consultation–AI consultation paired comparison, inter-brain/within-brain DLPFC metrics and robustness tests.
Neural–behavioural association and mediation analysis	Section 1.17	Synchrony–convergence correlation, AI → synchrony → convergence mediation path and Sobel test.
Surrogate controls and multiple comparisons	Section 1.19	Phase randomisation, cross-group random pairing, time shifting, empirical P values, z scores and BH-FDR.

All statistical analyses used the three-person team as the primary inference unit. Statistical notation was defined as

$$q = 1, \ldots, 32, \qquad C_q \in \{\mathrm{G0}, \mathrm{G1}, \mathrm{G2}, \mathrm{G3}\}, \qquad \mathcal{C}^{+} = \{\mathrm{G1}, \mathrm{G2}, \mathrm{G3}\}, \qquad r = 1, \ldots, 5, \qquad \tilde{r} = r - \bar{r}, \tag{65}$$

where q denotes team, C_q denotes experimental condition, $\mathcal{C}^{+}$ denotes the non-reference feedback conditions, r denotes round and $\tilde{r}$ denotes centred round. Behavioural total scores were first harmonised from role-side records to the team-by-round level:

$$Y_{q,r} = \frac{1}{|\mathcal{A}_{q,r}|} \sum_{a \in \mathcal{A}_{q,r}} Y_{q,r,a}, \tag{66}$$

where $\mathcal{A}_{q,r}$ is the set of available role-side records for the same team and round. Equations 65 and 66 define the team-level behavioural analysis unit. When the three role-side records corresponded to

the same jointly submitted solution, this average was used only to remove duplicate records and did not represent independent ratings by the three members.

Each team's convergence speed was defined as the ordinary-least-squares slope of round scores:

$$Y_{q,r} = \alpha_q + s_q r + \epsilon_{q,r}, \tag{67}$$

where s_q is the behavioural convergence slope of team q. Equation 67 underlies the behavioural slope values reported in Supplementary Table 1. Behavioural results report four main quantities: condition-wise round-mean trajectories, final-round performance, mean convergence slope and between-team dispersion. These summaries are the descriptive basis for the behavioural panels in the main text and are not duplicated elsewhere in the Supplementary Information. Sub-scores are used only to describe solution-quality composition and are not primary inferential outcomes.

Neural–behavioural association was analysed at the team level. Let $\bar{M}_q$ denote the team-level synchrony averaged across discussion-equivalent epochs, such as Pearson GS or WTC GS. The association between synchrony and convergence speed was reported as Spearman rank correlation:

$$\rho_{\mathrm{SB}} = \mathrm{corr}_{\mathrm{Spearman}}\left(\bar{M}_q, s_q\right). \tag{68}$$

Spearman correlation was the primary report because the sample size was the number of teams and the slope distribution could deviate from normality. Pearson correlation was used as a directional check.

Mediation analysis tested whether the paths among AI condition, inter-brain synchrony and behavioural convergence were consistent with an interpretation in which synchrony served as an intermediate process. Let

$$X_q = \mathbb{I}(C_q = \mathrm{G3}). \tag{69}$$

The three regression paths were

$$\bar{M}_q = \alpha_M + aX_q + \eta_q, \tag{70}$$

$$s_q = \alpha_Y + cX_q + \xi_q, \tag{71}$$

$$s_q = \alpha'_Y + c'X_q + b\bar{M}_q + \zeta_q. \tag{72}$$

The indirect effect was defined as $\hat{a}\hat{b}$, and the Sobel statistic was

$$z_{\mathrm{Sobel}} = \frac{\hat{a}\hat{b}}{\sqrt{\hat{b}^2\mathrm{SE}(\hat{a})^2 + \hat{a}^2\mathrm{SE}(\hat{b})^2}}. \tag{73}$$

Equations 69–73 define the mediation analysis. The behavioural-convergence, synchrony–slope and mediation analyses used an archived aligned team-by-round analysis table and archived inferential summaries. The corresponding synchrony–convergence, mediation, DLPFC and feedback-phase estimates are collated in Supplementary Table 2. Because the analysis unit was the team, statistical

power was limited. Mediation results were therefore interpreted as mechanism-consistency evidence rather than confirmatory causal evidence.

1.18 Inferential statistical models and effect sizes

This section corresponds to the static network inference, connection-category analysis, dynamic-state summary and within-G3 mechanistic tests reported in the main text. The corresponding numerical estimates are reported in Supplementary Tables 2 and 3, with robustness and surrogate-control summaries in Supplementary Table 4. All linear mixed-effects models used a team random intercept to account for repeated observations across rounds or epochs within the same team. Linear mixed-effects models were fitted with `statsmodels.formula.api.mixedlm` using restricted maximum likelihood; Kruskal–Wallis and pairwise non-parametric summaries used Pingouin/SciPy functions; rank correlations and paired tests used SciPy functions. The models used G0 as the no-feedback reference condition and centred round at round 3. Primary reported P values are two-sided, with a significance threshold of $\alpha = 0.05$; the one-sided Wilcoxon check is explicitly treated as a directional robustness check for the offloading prediction.

The primary model for static hyperbrain synchrony was

$$M_{q,r} = \beta_0 + \sum_{c \in \mathcal{C}^+} \beta_c \mathbb{I}(C_q = c) + \beta_r \tilde{r} + \sum_{c \in \mathcal{C}^+} \beta_{cr} \mathbb{I}(C_q = c)\tilde{r} + u_q + \epsilon_{q,r}, \tag{74}$$

where $M_{q,r}$ can be Pearson GS or WTC GS in the discussion-equivalent phase, $u_q \sim \mathcal{N}(0, \sigma_u^2)$ is the team random intercept and $\epsilon_{q,r}$ is the residual. G0 was the reference condition. Thus, β_{G3} represents the main effect of the AI-assisted group relative to the no-feedback group, and $\beta_{\mathrm{G3},r}$ represents the round-slope difference of the AI-assisted group relative to the no-feedback group.

To control residual differences in epoch duration, a sensitivity model added log duration:

$$M_{q,r} = \beta_0 + \sum_{c \in \mathcal{C}^+} \beta_c \mathbb{I}(C_q = c) + \beta_r \tilde{r} + \sum_{c \in \mathcal{C}^+} \beta_{cr} \mathbb{I}(C_q = c)\tilde{r} + \gamma \log(d_{q,r}) + u_q + \epsilon_{q,r}, \tag{75}$$

where $d_{q,r}$ is the duration of the corresponding discussion-equivalent phase. Equations 74 and 75 define the primary mixed-effects model and its duration-adjusted sensitivity model.

As a robustness test with weaker distributional assumptions, discussion-equivalent synchrony was first averaged across rounds within each team, followed by a Kruskal–Wallis test:

$$H = \mathrm{KW}\left(\bar{M}_q \mid C_q\right). \tag{76}$$

When the omnibus test suggested group differences, pairwise comparisons between conditions were performed and controlled using the Benjamini–Hochberg false-discovery-rate method.

The connection-category model tested whether synchrony enhancement was specific to homologous or complementary inter-brain edges. Let $h \in \{\mathrm{H}, \mathrm{C}\}$ denote connection type and $M_{q,r,h}$ the

corresponding strength. The model was

$$M_{q,r,h} = \beta_0 + \sum_{c\in\mathcal{C}^+} \beta_c \mathbb{I}(C_q = c) + \beta_h \mathbb{I}(h = \mathrm{H}) + \sum_{c\in\mathcal{C}^+} \beta_{ch} \mathbb{I}(C_q = c)\mathbb{I}(h = \mathrm{H}) + \beta_r \tilde{r} + u_q + \epsilon_{q,r,h}. \tag{77}$$

The key test in Eq. 77 was β_{ch}, the condition × connection-type interaction. A non-significant interaction did not support preferential concentration of the condition effect in homologous or complementary connections.

Inference on dynamic neural fingerprints proceeded in two steps. The first step was unsupervised HMM model selection and Viterbi decoding as described in Section 1.16, with state number determined by the BIC curve and model parsimony. The second step summarised the decoded state sequence into fractional occupancy, mean dwell time and switching rate at the team, condition or phase level; model-level transition entropy was reported as a descriptive property of the fitted HMM transition matrix. Because HMM states are latent dynamic patterns estimated jointly from all windows, the main text reports state-number selection, state stability and condition/phase-specific occupancy profiles. These results are interpreted as features of dynamic organisation rather than significance tests treating edges or windows as independent samples.

Within-G3 mechanistic tests compared pre-consultation discussion with AI consultation. For inter-brain DLPFC synchrony, let

$$D^{\mathrm{inter}}_{q,r} = \mathrm{IBS}^{\mathrm{DLPFC}}_{q,r,\mathrm{AI}} - \mathrm{IBS}^{\mathrm{DLPFC}}_{q,r,\mathrm{pre}}. \tag{78}$$

For within-brain DLPFC load, member and phase observations were first standardised within each team, and the AI consultation minus pre-consultation difference was then computed:

$$D^{\mathrm{intra}}_{q,r} = \tilde{L}^{\mathrm{DLPFC}}_{q,r,\mathrm{AI}} - \tilde{L}^{\mathrm{DLPFC}}_{q,r,\mathrm{pre}}. \tag{79}$$

The paired t-test statistic was

$$t = \frac{\bar{D}}{s_D/\sqrt{n}}, \qquad d_z = \frac{\bar{D}}{s_D}, \tag{80}$$

where D denotes the paired difference, s_D its standard deviation and d_z Cohen's d for a paired design. Within-brain load also used a one-sided Wilcoxon signed-rank test as a directional robustness check for the offloading prediction $D^{\mathrm{intra}}_{q,r} < 0$. The dissociation between inter-brain and within-brain changes was further evaluated by

$$\rho_\Delta = \mathrm{corr}\left(D^{\mathrm{inter}}, D^{\mathrm{intra}}\right). \tag{81}$$

Equations 78–81 define the within-G3 DLPFC dissociation tests. If inter-brain enhancement was not correlated with within-brain reduction, the simple offloading account was not supported.

Effect sizes for independent-group contrasts are reported as Cohen's d:

$$d = \frac{\bar{M}_1 - \bar{M}_0}{\sqrt{\frac{(n_1-1)s_1^2+(n_0-1)s_0^2}{n_1+n_0-2}}}, \tag{82}$$

where $\bar{M}_1$ and $\bar{M}_0$ are team-level means of the two groups. Equation 82 was used for independent-group contrasts, paired comparisons use d_z, and correlation analyses report ρ.

1.19 Surrogate controls, multiple comparisons and reporting rules

This section corresponds to the surrogate-control and multiple-comparison descriptions in the main-text statistical analysis. Surrogate controls were not intended to replace the primary models, but to compare observed synchrony with null distributions that preserved signal spectral structure, shared task timing or participant-level signal features.

The primary surrogate control was phase randomisation. Phase-randomisation, cross-team random-pairing, temporal-shift and two-level surrogate summaries were computed as archived robustness outputs. For each team, member, ROI and epoch, the time series was Fourier transformed, and phases were randomised while preserving the amplitude spectrum:

$$\tilde{X}^{(m)}(f) = |X^{(m)}(f)|e^{i\phi_{\mathrm{rand}}(f)}, \qquad \phi_{\mathrm{rand}}(f) \sim \mathrm{Uniform}(0, 2\pi). \tag{83}$$

An inverse transform then produced surrogate time series, and synchrony metrics were recomputed. Each observation was repeated $B = 1{,}000$ times, forming the surrogate distribution $\{M_{\mathrm{surr}}^{(b)}\}_{b=1}^{B}$. The standardised score of the observed value relative to the surrogate distribution was

$$z_{\mathrm{surr}} = \frac{M_{\mathrm{true}} - \mu_{\mathrm{surr}}}{\sigma_{\mathrm{surr}}}, \tag{84}$$

where μ_{surr} and σ_{surr} are the mean and standard deviation of the surrogate distribution. The empirical upper-tail P value was

$$P_{\mathrm{emp}} = \frac{1 + \sum_{b=1}^{B} \mathbb{I}\left(M_{\mathrm{surr}}^{(b)} \geq M_{\mathrm{true}}\right)}{B+1}. \tag{85}$$

Equations 83–85 define the phase-randomisation surrogate and its empirical significance test.

The second surrogate control was cross-group random pairing. This procedure recombined members from different real teams into pseudo-triads while preserving role structure, and then recomputed inter-brain synchrony. This control compared observed G3 synchrony with the random-pairing null distribution, providing a conservative check on whether participant-level average signal features alone could account for the observed pattern.

The third surrogate control was time shifting. One member's ROI time series was circularly shifted by 5–30 s, and inter-brain synchrony was recomputed. This procedure preserves single-person autocorrelation structure and overall spectral features but disrupts real temporal alignment

in interaction. A reduction after time shifting would be consistent with a dependence on real temporal coupling. Surrogate controls were used to define the interpretive boundaries of synchrony, not to replace the primary model. Robustness and surrogate-control results are summarised in Supplementary Table 4; the distributional diagnostics for phase randomisation, time shifting and cross-team pairing are shown in Supplementary Fig. 2.

Multiple comparisons were controlled by analysis family. Predefined primary model parameters included the G3-versus-G0 main effect on GS, the G3 $\times$ round interaction, the within-G3 change in inter-brain DLPFC synchrony during AI consultation relative to pre-consultation, and the within-brain DLPFC load change. Exploratory or pairwise condition comparisons used Benjamini–Hochberg FDR correction with $q = 0.05$. The main text reports exact P values; very small values are reported as $P < 0.001$. All figure error bars and distribution plots use team-level observations, not members, channels or edges as independent samples.

Supplementary Figures

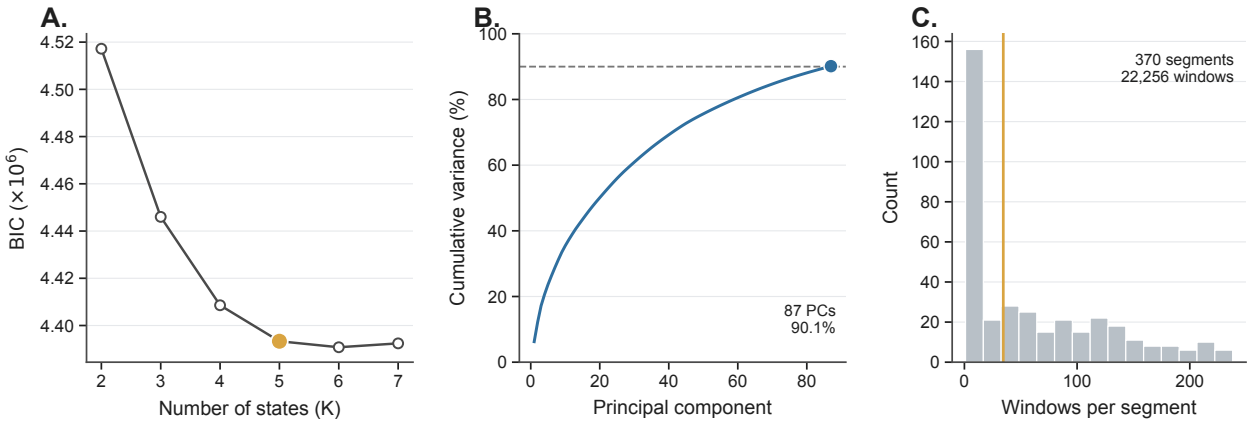

Supplementary Figure 1: Hidden Markov model diagnostic summaries. **a**, BIC curve across candidate state numbers. The retained five-state model is highlighted in orange as the elbow-and-parsimony solution, although the six-state model had a marginally lower absolute BIC. **b**, Cumulative PCA variance retained before HMM fitting. **c**, Distribution of segment lengths entering the HMM, expressed as sliding-window counts.

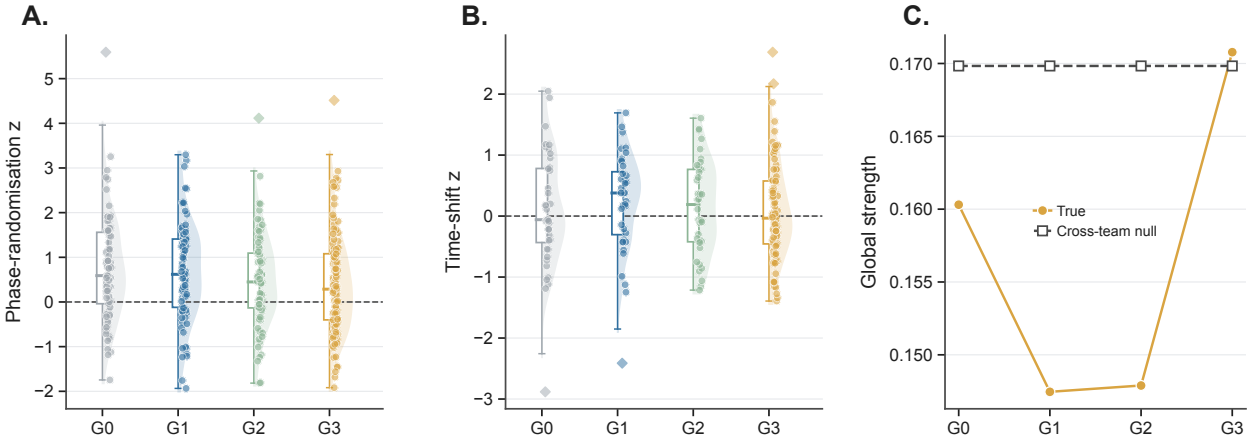

Supplementary Figure 2: Surrogate-control diagnostic summaries. **a**, Phase-randomisation z scores by condition. **b**, Time-shift z scores by condition. **c**, True condition-level global strength compared with the cross-team random-pairing null. These diagnostics are used to define the interpretive boundaries of synchrony rather than as additional primary endpoints.

Supplementary Tables

Supplementary Table 1: Behavioural performance across the four experimental conditions.

Group	R1	R2	R3	R4	R5	Slope	Slope SD
G0	29.4	26.6	33.3	47.2	49.4	6.07	8.30
G1	31.6	37.0	49.5	57.3	59.2	7.55	4.66
G2	29.1	36.6	53.7	64.8	68.1	10.62	4.50
G3	29.0	50.5	59.1	67.6	68.7	9.66	2.88

Note. R1–R5 are condition-level means of team total score by round, computed from the team-level behavioural table after harmonising duplicate role-side records. Slope is the ordinary-least-squares score change per round for each team, averaged within condition; Slope SD is the between-team standard deviation of those slopes. Each condition contains eight teams.

Supplementary Table 2: Selected inferential results for global synchrony, convergence and DLPFC dissociation.

Analysis	Contrast or path	Statistic	P
Pearson global strength	G3 relative to G0	$\beta = 0.047$, $d = 1.79$	0.001
Pearson global strength with duration covariate	G3 relative to G0	$\beta = 0.049$	< 0.001
WTC global strength	G3 relative to G0	$\beta = 0.0036$, $d = 1.98$	0.0001
WTC round interaction	G3 by round interaction	$\beta = 0.0012$	0.0007
Connection-category interaction, Pearson	Group × connection type	$\beta = 0.0004$	0.970
Connection-category interaction, WTC	Group × connection type	$\beta = 0.0001$	0.880
Convergence correlation, Pearson GS	GS and slope	$\rho = 0.238$	0.189
Convergence correlation, WTC GS	WTC GS and slope	$\rho = 0.180$	0.325
Mediation path a	LLM condition → synchrony	$\beta = 0.043$	0.0006
Mediation indirect effect	LLM condition → synchrony → slope	Sobel $z = 0.71$	0.478
DLPFC load, offloading check	AI minus pre, directional check AI < pre	$t = 0.379$, $d_z = 0.07$	0.707
Inter-brain DLPFC, Pearson	AI relative to pre	$t = 3.33$, $d_z = 0.58$	0.002
Inter-brain DLPFC, WTC	AI relative to pre	$t = 4.39$, $d_z = 0.76$	0.0001
Inter/within DLPFC dissociation	Within-change versus inter-change	$\rho = 0.030$	0.870
Feedback-phase synchrony	G2 relative to G3	$U = 12.0$, $d = 0.70$	0.038
G3 feedback relative to discussion	Feedback relative to pre-consultation	$t = 18.52$, $d_z = 7.29$	< 0.001

Note. Mixed-model β estimates are fixed effects with G0 as the no-feedback reference condition unless the contrast states otherwise. Pre denotes the pre-consultation phase. d denotes independent-group Cohen's d; d_z denotes paired Cohen's d; U denotes the Mann–Whitney statistic; ρ denotes Spearman rank correlation. Results are team-level or team-by-round analyses, not member-, channel- or edge-level independent tests.

Supplementary Table 3: Summary of hidden Markov model results.

Metric	Value
Selected state number	$K = 5$, determined from the BIC curve elbow and model parsimony
BIC curve	$K = 2$: 4,517,200; $K = 3$: 4,445,997; $K = 4$: 4,408,575; $K = 5$: 4,393,339; $K = 6$: 4,390,795; $K = 7$: 4,392,437. Marginal improvement decreased markedly after $K = 5$, and $K = 7$ rebounded.
PCA reduction	87 components retained, explaining 90.1% of variance
Total dynamic segments	370
Total windows	22,256
Model-level transition entropy	4.491
Self-transition range	0.832–0.872
Dominant discussion state by group	G0: state 4 (36.3%); G1: state 3 (28.4%); G2: state 1 (31.2%); G3 pre-consultation: state 2 (27.8%)
AI consultation-specific occupancy profile	State 4 = 38.7%; state 0 = 8.2%; state 2 = 18.8%

Note. HMM inputs were 147-edge sliding-window connectivity vectors reduced to 87 principal components. BIC values are reported for the full-covariance Gaussian HMMs fitted with 10 restarts per K. $K = 5$ was retained as an elbow-and-parsimony solution; the lower absolute BIC at $K = 6$ is reported in the curve so that the selection rule is auditable. State numbers are data-driven labels and should not be read as fixed psychological categories.

Supplementary Table 4: Summary of robustness and surrogate-control analyses.

Analysis	Main result	Interpretive boundary
Duration-covariate model	The G3-versus-G0 Pearson global-strength effect remained significant, $\beta = 0.049$, $P < 0.001$; the log-duration covariate was $\beta = -0.087$, $P < 0.001$.	The G3-versus-G0 effect was robust to adjustment for residual epoch-duration differences.
Non-parametric condition test	Pearson global strength: Kruskal–Wallis $H = 10.78$, $P = 0.013$; WTC global strength: $H = 13.78$, $P = 0.003$.	Condition differences remained observable under tests with weaker distributional assumptions.
Connection-category interaction	In Pearson, the G3 × homologous interaction was $\beta = 0.0004$, $P = 0.970$; the corresponding WTC interaction was $\beta = 0.0001$, $P = 0.880$.	The LLM effect is not supported as a local enhancement of a specific homologous or complementary edge category.
Phase-randomisation control	Mean team-level surrogate score was $z = 0.212$, $t = 2.86$, $P = 0.007$; Wilcoxon $P = 0.006$; between-group comparison $H = 1.05$, $P = 0.790$.	Observed synchrony was overall higher than a phase-randomised null preserving spectral structure, but this summary does not support attributing surrogate-score differences to a single condition.
Cross-team random pairing	The true G3 mean was 0.1708, the cross-team random-pairing mean was 0.1698, $z = 0.098$, $P = 0.461$.	This conservative control did not show that G3 was higher than the random-pairing null at the group level; the main conclusion does not rely on this surrogate test.
Time-shift control	Across 216 discussion epochs, the number of significant time-shift surrogate tests after BH-FDR correction was 0.	Time-shift results did not add single-epoch FDR-significant support and are used to limit, not strengthen, causal interpretation.

Note. Robustness analyses were designed to bound interpretation rather than to create additional primary endpoints. The duration model tests residual epoch-length confounding; non-parametric tests summarise team-averaged condition differences; surrogate controls preserve different nuisance structures while disrupting different forms of coupling. Negative or conservative surrogate findings are retained because they define the limits of the synchrony interpretation.

References

[1] Fishburn, F. A., Ludlum, R. S., Vaidya, C. J. & Medvedev, A. V. Temporal derivative distribution repair (TDDR): a motion correction method for fNIRS. *Neuroimage* **184**, 171–179 (2019). https://doi.org/10.1016/j.neuroimage.2018.09.025

[2] Yang, M. & Wang, J. *Ship Aesthetics and Cabin Design* (in Chinese). Beijing: Science Press

(2021). ISBN 9787030673954.

[3] Yang, D. *Research and Design of Ship Cabin Environmental Engineering* (in Chinese). Harbin: Harbin Engineering University Press (2020). ISBN 9787566126450.

[4] Kocsis, L., Herman, P. & Eke, A. The modified Beer–Lambert law revisited. *Phys. Med. Biol.* **51**, N91–N98 (2006). https://doi.org/10.1088/0031-9155/51/5/N02

[5] Tzourio-Mazoyer, N. *et al.* Automated anatomical labeling of activations in SPM using a macroscopic anatomical parcellation of the MNI MRI single-subject brain. *Neuroimage* **15**, 273–289 (2002). https://doi.org/10.1006/nimg.2001.0978

[6] Rolls, E. T., Huang, C.-C., Lin, C.-P., Feng, J. & Joliot, M. Automated anatomical labelling atlas 3. *Neuroimage* **206**, 116189 (2020). https://doi.org/10.1016/j.neuroimage.2019.116189

[7] Singh, A. K., Okamoto, M., Dan, H., Jurcak, V. & Dan, I. Spatial registration of multichannel multi-subject fNIRS data to MNI space without MRI. *Neuroimage* **27**, 842–851 (2005). https://doi.org/10.1016/j.neuroimage.2005.05.019

[8] Tsuzuki, D., Jurcak, V., Singh, A. K., Okamoto, M., Watanabe, E. & Dan, I. Virtual spatial registration of stand-alone fNIRS data to MNI space. *Neuroimage* **34**, 1506–1518 (2007). https://doi.org/10.1016/j.neuroimage.2006.10.043

[9] Grinsted, A., Moore, J. C. & Jevrejeva, S. Application of the cross wavelet transform and wavelet coherence to geophysical time series. *Nonlinear Process. Geophys.* **11**, 561–566 (2004). https://doi.org/10.5194/npg-11-561-2004

Appendix A: English Translation of the Participant Recruitment Notice

Note: This appendix is a de-identified English translation of the participant recruitment notice. Direct contact details, registration links, payment-processing information and other identifying metadata have been removed.

Recruitment: Three-person Group Decision-making Experiment on Luxury Cruise Cabin Design with fNIRS Brain Imaging

Compensation: Participants were compensated according to the ethics-approved study protocol. If a participant withdrew before completion, compensation was prorated according to completed participation.
Research unit: Research team at the School of Mechanical Engineering, Shanghai Jiao Tong University.
Study title: Three-person interdisciplinary group decision-making intervention experiment, using a luxury cruise cabin design task with fNIRS hyperscanning.
Location: Shanghai Jiao Tong University.
Duration: Approximately 90–120 minutes per session, including preparation, device setup and questionnaire completion.
Recruitment target: 96 participants in total, corresponding to four paradigms, eight groups per paradigm and three participants per group, for 32 sessions in total.
Payment: Compensation was provided after participation according to the approved protocol. Participants who withdrew midway were compensated in proportion to the completed part of the experiment.

1. What Are We Studying?

We compare how different timings and forms of human–AI intervention affect three-person collaborative design:

- G0, no intervention: discussion → submission. The system scores the design but does not display the score to participants.
- G1, end-of-round feedback: discussion → submission → score interval, viewed silently.
- G2, end-of-round explanatory feedback: discussion → submission → score interval plus rule conflicts and trade-off suggestions.
- G3, three-stage procedure: discussion → AI consultation → submission → score plus rules.

Each group completes five rounds and selects a final solution. At the same time, participants wear fNIRS caps, which use non-invasive near-infrared light, to record brain activity and group synchrony.

2. Who Are We Looking For?

Basic criteria, all of which must be satisfied:

- Senior undergraduate students or master's/doctoral students in relevant majors, aged 18–35 years, Mandarin-speaking, right-handed and right-eye dominant.
- Participants from the following three disciplinary areas:

1. Ship structural field

- Holds or is about to obtain a bachelor's, master's or doctoral degree in engineering mechanics, naval architecture and ocean engineering, or a related discipline, and has participated in project design work related to ship cabin design.
- Has practical experience in structural analysis and design, including use of relevant software such as SAP2000, ETABS or ANSYS.
- Has systematically studied the following courses: theoretical mechanics; mechanics of materials; and at least one of structural mechanics, structural dynamics or principles of structural design.

2. Environmental engineering field

- Holds or is about to obtain a bachelor's, master's or doctoral degree in environmental science, environmental engineering, environmental science and engineering, or a related discipline, and has participated in project design work related to ship cabin design.
- Has systematically studied the following courses: principles of environmental engineering; environmental monitoring or environmental monitoring experiments; and environmental planning and management.

3. Aesthetics/design field

- Holds or is about to obtain a bachelor's, master's or doctoral degree in environmental design, art design or a related discipline, and has participated in project design work related to ship cabin design.
- Has practical experience in engineering design, including use of design-related software such as AutoCAD, SketchUp or Adobe Creative Suite.
- Has systematically studied the following courses: decorative materials and construction; interior environmental design; and design drafting and perspective.

Participants must be willing to wear an fNIRS cap and accept full-session audio recording, which is used only for behavioural coding and will not be disseminated. Participants should have normal or corrected-to-normal vision, be able to tie up their hair as required, and be able to remove thick hats or hair accessories. Participants must sign the informed consent form and privacy statement. Participants must be right-handed.

Exclusion criteria, any one of which precludes participation:

- Scalp inflammation or recent scalp injury, or extremely thick or unmanageable hair that prevents probe contact.
- Sensitivity to bright light or screen flicker, self-reported history of epilepsy, or current use of strong sedative or stimulant medication.
- A superior–subordinate or intimate relationship with another participant in the same session.
- Prior participation in the formal experiment or pilot experiment of this study.

Each three-person group has fixed roles, with one participant each for structure (S), aesthetics (A) and environment (E). Groups are formed according to registration information. On arrival, each participant's role is consistent with their primary background.

3. What Will You Do in the Experiment?

- Read the task brief for a luxury cruise cabin design decision scenario and adjust 15 design control items in a graphical user interface.
- In each discussion round, speak in the order structure → aesthetics → environment. Each speaker has no more than 90 seconds. If there is no new opinion, say "pass". Interruptions are not allowed.
- After each speaking cycle, there is a short editing window. Only the operator for the current round implements the agreed modifications in the interface.
- Depending on group assignment, participants may see scores, rules, conflict explanations or trade-off suggestions at the end of each round, or may consult the AI during the round.
- After five rounds, the final solution is locked. Participants then complete questionnaires, including TLX, satisfaction/fairness/trust measures, and leave after receiving compensation.

4. Schedule and Quotas

There are 32 sessions in total, with three participants per session: G0, 8 sessions and 24 participants; G1, 8 sessions and 24 participants; G2, 8 sessions and 24 participants; G3, 8 sessions and 24 participants. Morning and afternoon sessions were available. Condition assignment followed the approved study schedule and balancing requirements.

5. Compensation and Withdrawal

Compensation was provided according to the approved protocol after completion. If a participant withdrew midway, payment was made in proportion to the completed part. Participants arriving more than 10 minutes late might not be able to participate. Participants were asked to arrive 5–10 minutes early when possible. Participants could withdraw or request a pause at any time.

6. Data and Privacy

Data collected include GUI operation logs, rounds and timestamps, audio recordings for transcription and speaking-time statistics, and raw and processed fNIRS indices. Data are stored using de-identified IDs; the linkage table is encrypted and stored separately. Only authorised research personnel have access. With separate consent, we may publicly release a de-identified dataset in an academic repository. Such a dataset will not contain raw audio/video, facial information or the linkage table. The study was approved by the Shanghai Jiao Tong University Ethics Review Committee for Science and Technology Research Involving Human Participants, with ethics approval number I20250750I, and was conducted according to the approved requirements.

7. Registration

Registration involved two steps. First, participants completed an online registration and screening form taking approximately 2–3 minutes. The form collected only information necessary for eligibility screening and scheduling, including disciplinary background, relevant experience, available time slots, health and exclusion information, and optional consent preferences. Second, the research team confirmed eligibility and group assignment. Participants were paired into groups according to structural, aesthetic and environmental backgrounds and contacted through approved study channels to confirm the session, location and precautions. Those not selected entered a waiting list.

On arrival, participants should bring a valid identity or institutional document required by site procedures for sign-in and compensation receipt. Participants are advised to wash their hair the night before the experiment. Clothing and hairstyle should allow cap placement; thick hats or complex hair accessories should be avoided, and long hair may be tied up.

8. Notes

Participants should follow the turn-taking and speaking-time rules throughout the experiment. During discussion, they may not operate the GUI; only the operator for the current editing window may do so. Participants may report discomfort at any time, such as cap pressure marks, heat or fatigue. Large luggage and drinks should not be brought into the experimental area. Mobile phones should be set to silent mode.

9. Organisation and Quota Summary

The paradigms and quotas are: G0–G3, eight groups each; three participants per group; 32 groups and 96 participants in total. Each session lasts 90–120 minutes. Compensation was provided according to the approved protocol.

10. Frequently Asked Questions

Q1. Is fNIRS safe? Does it involve radiation?

fNIRS uses low-intensity near-infrared light. It is non-ionising and non-invasive and is commonly

used in human factors and cognitive research. Mild pressure marks or heat may occur, and the device can be adjusted or the experiment paused at any time.

Q2. Must I know ship design?

Real project experience is not strictly required. Coursework foundations in structure, aesthetics or environment are sufficient. Relevant background materials will be provided before participation, and interface operation will be trained on site.

Q3. What if a group member is absent?

A waiting list is maintained. If a replacement cannot be arranged on site, the session will be rescheduled to the nearest available time.

Q4. Can I choose which paradigm to join?

No. Participants are assigned to one of the paradigms G0–G3 according to the approved study schedule and balancing requirements.

Appendix B: English Translation of the Informed Consent Form

Note: This appendix is a de-identified English translation of the informed consent form. Version metadata, direct contact details, payment-processing details and other identifying metadata have been removed.

Informed Consent Form

Project title: Multi-objective collaborative decision-making and human–AI intervention in complex engineering domains: mechanisms, methods and platform.
Ethics approval number: I20250750I.
Research institution: Department of Industrial Engineering and Management, School of Mechanical Engineering, Shanghai Jiao Tong University.
Funding source: Research on the mechanism and intervention strategies of interdisciplinary group decision-making in engineering fields based on neurocognitive methods, No. 72271163.

1. Study Description: Purpose, Content and Timeline

We are conducting a non-invasive behavioural study on the role of AI advice in team collaboration. You will be invited to complete a five-round collaborative design task on a computer together with two other participants. Each round lasts approximately 8–10 minutes. Depending on the condition, you may receive AI advice in real time, after a round, or not at all. To understand the collaboration process, we will record dialogue audio for local transcription, operation logs and non-invasive fNIRS near-infrared brain oxygenation signals. One full participation session lasts approximately 90–120 minutes. The study period is October 2025 to March 2026, and the planned sample size is approximately 96 participants.

2. Research Team and Qualifications

The study is conducted by a research team in the Department of Industrial Engineering and Management, School of Mechanical Engineering, Shanghai Jiao Tong University. The researchers have completed training in human participant research ethics, science and technology ethics, and personal information protection, and have passed relevant operational and safety assessments. Qualification and training certificates can be provided for inspection when necessary.

3. Participation Requirements: Inclusion and Exclusion

Inclusion criteria are: 18–35 years old, right-handed, right-eye dominant, normal hearing and vision, ability to communicate normally in Chinese, and physical condition sufficient to complete an indoor task lasting approximately 1.5–2 hours.

Exclusion criteria are: obvious discomfort on the day of the experiment; allergy to scalp-contact materials or intolerance of fNIRS; recent major emotional distress; prior participation in this study;

or any other condition judged by the researcher to make participation unsuitable.

4. What Participation Involves and Notes

The procedure is: arrival → screening and consent → device placement → 30-second resting baseline and 5-minute task-material reading → task demonstration → formal five-round task → questionnaires and brief interview → data check and compensation.

Participants may bring or be provided with a hair band or disposable liner and should maintain a comfortable sitting posture where possible. If you feel uncomfortable, nervous or involved in a dispute, you may immediately notify the researcher and pause the experiment. You have the right to refuse to answer any question or stop any step.

5. Possible Risks and Protections

Possible discomforts or risks include mild scalp pressure marks or heat, short-term tension or emotional fluctuation, a low-probability risk of privacy leakage, and the possibility that AI advice may influence the direction of discussion.

Protective measures include the following. The equipment is non-invasive and non-ionising. Devices are strictly disinfected and wearing time is limited, with each session lasting no more than 120 minutes and breaks of 1–2 minutes between rounds. Data are stored in de-identified form, with identity and code information separated and encrypted. The AI consultation module was operated through the approved study interface, with usage limits and an emergency stop. If discomfort occurs, the participant may pause or withdraw at any time, and the event will be recorded and handled.

6. Possible Benefits

Direct benefits include compensation according to the approved protocol, experience with collaboration and decision-making, and opportunities to improve self-reflection and communication awareness. Participants may choose to receive a group-level summary of results.

Social and academic benefits include contributing to fairer and more efficient methods for human–AI collaboration, with potential applications in engineering collaboration, education and training.

7. Voluntary Participation and Withdrawal

Participation is entirely voluntary. You may withdraw at any stage, at any time and for any reason, and you will not receive unfair treatment or adverse consequences as a result. Upon withdrawal, identifiable information that has already been generated will be deleted or destroyed. De-identified data that can no longer identify you may be used for statistical research in accordance with law. Compensation will be settled according to completed participation under the approved protocol.

8. Alternatives

If you are unwilling to wear fNIRS, you may decline participation, request rescheduling or receive only the group-level research summary. These choices do not affect participant rights, and any compensation followed the approved protocol.

9. Costs, Compensation and Treatment of Research-related Injury

Participation is free of charge. Compensation and any eligible travel reimbursement are provided according to the approved protocol, with payment records retained as required by institutional procedures.

The study is minimal risk. If unexpected discomfort or harm is caused by the research procedure, the research team and institution will respond according to institutional procedures and applicable regulations.

10. Information Use, Confidentiality, Sharing and Secondary Use

Only the minimum information necessary for scheduling and statistical analysis will be collected. Upon storage, participant identity is replaced with a participant code. The identity–code mapping table is stored separately and encrypted.

Data are used only for the predetermined scientific purposes of this project and for necessary audit checks, such as inspections by the university, regulators or ethics committee in accordance with regulations. Publications will present only de-identified group statistics and methods.

De-identified data will be stored for five years. The mapping table will be stored until one year after the end of the study or until audit completion, and then deleted. Upon expiry, materials will be irreversibly destroyed according to institutional procedures and the destruction will be documented.

Identifiable data are not shared externally by default. If future secondary research related to this topic is proposed, anonymous or de-identified data will be used, and additional ethics approval and renewed explicit consent will be obtained.

11. Notification of New Information and Re-consent

If new information or protocol revisions arise during the study that may affect your decision to continue participation, we will inform you promptly and, where necessary, invite you to sign an updated consent form.

12. Study Time and Number of Participants

The study is planned for October 2025 to March 2026 and will recruit 96 participants, with three participants per group.

13. Feedback and Publication of Results

Study results will be published in journals, conferences or similar venues. Participants who subscribe will receive a PDF and link to a group-level result summary by email. No individual diagnosis or identifiable data will be provided.

14. Biological Samples

The study does not involve collection, storage or external provision of human biological samples. If biological samples are involved in the future, separate ethics approval and renewed consent will be obtained.

15. Contact Information

Research, adverse-event, ethics and privacy enquiries were handled through institutionally approved study contact channels provided to participants during recruitment and consent.

Researcher Statement

"I have fully explained to the research participant the background, purpose, procedures, possible risks and benefits of this study, allowed sufficient time for the participant to read this consent form, and answered relevant questions. I have clearly explained that participation is voluntary and that the participant may withdraw at any time. I have also informed the participant of the research and ethics contacts. I confirm that I will provide the participant with a signed copy of this consent form."
Researcher signature: _____ Date: _____ year ____ month ____ day

Participant Statement

"I have read and understood the above content, and the researcher has answered my questions. I understand that participation is entirely voluntary and that I may withdraw at any time without reason and without adverse consequences. I agree to participate in this study as described in this informed consent form and have received a signed copy of this document."
Participant signature: _____ Date: _____ year ____ month ____ day
If applicable, legal representative signature: _____
Relationship to participant: _____ Date: _____ year ____ month ____ day

Appendix C: English Translation of the Ethics Approval Document

Note: This appendix is a de-identified English translation of the ethics approval document. Form metadata, internal review sequence numbers, personal names, direct committee contact details and other identifying metadata have been removed.

Ethics Review Approval

Committee: Shanghai Jiao Tong University Ethics Review Committee for Science and Technology Research Involving Human Participants.
Document title: Ethics Review Approval.
Statement: This ethics review committee is constituted and operates with reference to relevant national laws and regulations and relevant regulations of Shanghai Jiao Tong University. Its review and work processes are not influenced by any organisation or individual outside this committee.
Approval number: I20250750I.
Review location: Shanghai Jiao Tong University.
Project title: Research on mechanisms and intervention strategies for interdisciplinary group decision-making in engineering fields based on neurocognitive methods.

Review Documents

1. Application for an ethics project involving human participants in science and technology research, including overview of scientific and technological activities, funding source, commitment letter and scientific justification.
2. Research protocol, including implementation plan, research experience, risk prevention and control, emergency plan, and form of results release.
3. Informed consent form.
4. Project approval notice.
5. Project plan.
6. Project application.
7. Curriculum vitae of the project leader.
8. Researchers' financial interest statement.
9. Instrument safety certificate.

Research department: School of Mechanical Engineering.
Approved sample size: The approved sample size covered the analysed sample reported in this study.

Review method: Expedited review. According to the Measures for Ethical Review of Science and Technology (Trial), Guo Ke Fa Jian [2023] No. 167, and this committee's operating procedures, the project meets the category of minimal risk.

Review Opinions

1. The Shanghai Jiao Tong University Ethics Review Committee for Science and Technology Research Involving Human Participants reviewed the project and agreed that the project may be conducted.

2. The committee will conduct annual/periodic follow-up review of the research implementation process, with the frequency counted from the date of study approval: 12 months.

3. The institutional ethics committee has the right to change the frequency of annual/periodic follow-up review according to actual progress.

4. The approval is valid for one year from the date of approval.

Approval record: The document was signed and stamped by the Shanghai Jiao Tong University Ethics Review Committee for Science and Technology Research Involving Human Participants.

Notes

1. The project approved by the committee is a science and technology research activity involving human participants. It must be conducted strictly according to the latest approved versions of the research protocol and informed consent form, and must comply with relevant domestic laws, regulations and guidelines.

2. Any content involving export of human genetic resources or requiring special approval by relevant departments under national regulations must be reported to the relevant departments and approved before implementation. Projects that fall within the list of scientific and technological activities requiring ethics review re-examination must obtain approval from the re-examination expert group before implementation.

3. Collaborative projects should be conducted only after science and technology ethics review or written approval by the countries and institutions of all collaborating parties. This approval document may be used as a reference for other ethics committees. If there are different opinions regarding protocol review, please communicate with this committee in a timely manner.

4. Any modifications to approved research protocols, informed consent forms and other materials, and any change of principal investigator, must be reported promptly to the institutional ethics committee for re-review and may be implemented only after approval.

5. Serious adverse events and unexpected events that affect the risk–benefit ratio of the study must be reported promptly to the institutional ethics committee.

6. According to the committee's opinion on the frequency of annual/periodic follow-up review, regardless of whether the study has begun, an application for annual/periodic follow-up review must be submitted one month before the annual/periodic follow-up review due date.

7. Any non-compliance or protocol violation must be reported promptly to the ethics committee for review.

8. If the study is suspended or terminated early, the institutional ethics committee must be notified promptly.

9. Upon completion of the study, a final report must be submitted to the institutional ethics committee for review.

Appendix D: Task Scoring Parameters and Benchmark-Solution Calculation

This appendix lists the cost, weight and itemised benchmark-solution calculations used in the task scoring function. All values are internal relative units used to keep solution comparisons consistent within the same experimental paradigm; they should not be interpreted as real ship-construction costs or physical weights.

D.1 Cost and weight mappings

Param.	**Cost function** $c_i(p_i)$	**Weight function** $w_i(p_i)$
S1	$c(0.3) = 80,\ c(0.6) = 120,\ c(0.9) = 200$	$w(0.3) = 150,\ w(0.6) = 130,\ w(0.9) = 90$
S2	$60p_{S2}$	$25p_{S2}$
S3	$c(0.3) = 30,\ c(0.6) = 50,\ c(0.9) = 80$	$w(0.3) = 30,\ w(0.6) = 50,\ w(0.9) = 80$
A1	$c(0.3) = 40,\ c(0.6) = 90,\ c(0.9) = 180$	$w(0.3) = 20,\ w(0.6) = 60,\ w(0.9) = 130$
A2	$50p_{A2}$	$20p_{A2}$
A3	$-30p_{A3}$	$-40p_{A3}$
E1	$c(0.3) = 60,\ c(0.6) = 100,\ c(0.9) = 150$	$w(0.3) = 10,\ w(0.6) = 20,\ w(0.9) = 30$
E2	$c(0.3) = 0,\ c(0.6) = 20,\ c(0.9) = 50$	$w(0.3) = 0,\ w(0.6) = -5,\ w(0.9) = -10$
E3	$c(0.3) = 10,\ c(0.6) = 25,\ c(0.9) = 50$	$w(0.3) = 5,\ w(0.6) = 10,\ w(0.9) = 15$
SA1	$70p_{SA1}$	$-8p_{SA1}$
SA2	$c(0.3) = 20,\ c(0.6) = 50,\ c(0.9) = 100$	$w(0.3) = 10,\ w(0.6) = 30,\ w(0.9) = 60$
SE1	$c(0.3) = 30,\ c(0.6) = 60,\ c(0.9) = 110$	$w(0.3) = 20,\ w(0.6) = 40,\ w(0.9) = 70$
SE2	$c(0.3) = 20,\ c(0.6) = 60,\ c(0.9) = 120$	$w(0.3) = 15,\ w(0.6) = 40,\ w(0.9) = 80$
AE1	$c(0.3) = 20,\ c(0.6) = 50,\ c(0.9) = 90$	$w(0.3) = 10,\ w(0.6) = 30,\ w(0.9) = 60$
AE2	$c(0.3) = 30,\ c(0.6) = 60,\ c(0.9) = 100$	$w(0.3) = 5,\ w(0.6) = 10,\ w(0.9) = 20$

D.2 Cost and weight calculation for the benchmark solution

Param.	**Value**	**Meaning**	**Cost**	**Weight**
S1	0.90	Fibre-reinforced composite	200.0	90.0
S2	0.00	Compact-column endpoint	0.0	0.0
S3	0.30	Single-layer integrated panel	30.0	30.0
A1	0.30	Industrial coating	40.0	20.0
A2	0.01	Near the geometric-minimal endpoint	0.5	0.2
A3	0.55	Moderate openness	-16.5	-22.0
E1	0.60	Heat-recovery system	100.0	20.0
E2	0.60	Mixed recycled material	20.0	-5.0
E3	0.90	Touchless water outlet	50.0	15.0
SA1	0.00	Porthole-series endpoint	0.0	0.0
SA2	0.30	Hidden integration	20.0	10.0
SE1	0.60	Double-layer insulation	60.0	40.0
SE2	0.90	Enhanced zoning	120.0	80.0
AE1	0.60	Zoned absorption	50.0	30.0

AE2	0.30	Cool-white LED	30.0	5.0
Total			**704.0**	**313.2**

D.3 Domain-score calculation for the benchmark solution

Param.	**Structural contribution**	**Aesthetic contribution**	**Environmental contribution**
S1	16.20	10.80	1.00
S2	14.00	0.00	6.00
S3	4.80	7.00	4.20
A1	5.60	6.00	7.00
A2	4.95	0.13	4.95
A3	3.60	7.70	3.60
E1	1.60	5.40	7.20
E2	7.00	3.60	8.40
E3	0.00	7.00	7.20
SA1	8.00	0.00	8.00
SA2	5.60	3.30	3.50
SE1	6.60	2.80	6.00
SE2	10.80	0.90	5.40
AE1	1.60	6.60	3.60
AE2	0.00	2.70	4.20
Base score	**90.35**	**63.93**	**80.25**
Conflict penalty	0.00	0.00	0.00
Domain score	**90.35**	**63.93**	**80.25**

The benchmark solution triggers no second-order conflict penalty, and neither cost nor weight exceeds its constraint upper bound. The soft penalty is therefore 0. The total score is

$$T = \mathrm{clip}_{0,100}\left[\frac{90.35 + 63.93 + 80.25}{3}\right] = 78.18. \tag{86}$$

Appendix E: fNIRS Channel MNI Coordinates and ROI Mapping

This appendix lists the MNI standard-space coordinates of the 26 fNIRS channels, the corresponding AAL3 anatomical regions, Brodmann areas (BAs) and the functional ROIs used in this study. Coordinates are in mm. Positive X indicates right, positive Y indicates anterior and positive Z indicates superior. AAL3 labels were used for anatomical localisation, whereas functional ROIs were used for hyperbrain graph node aggregation in the main text.

Channel	X	Y	Z	AAL3 region	BA	ROI
Fpz_Fp1	-14.67	86.09	-4.35	Frontal_Sup_2_L	BA 10	FPA
Fpz_Fp2	14.99	86.58	-4.39	Frontal_Sup_2_R	BA 10	FPA
AF7_Fp1	-42.14	76.25	-8.79	Frontal_Mid_2_L	BA 9/46	DLPFC
AF8_Fp2	42.80	77.28	-8.92	Frontal_Mid_2_R	BA 9/46	DLPFC
Fpz_AFz	0.17	84.51	16.86	Frontal_Sup_Medial_R	BA 9/10	mPFC
AF3_Fp1	-31.57	80.38	7.12	Frontal_Sup_2_L	BA 10	FPA
AF7_AFF5h	-52.82	66.31	6.25	Frontal_Mid_2_L	BA 9/46	DLPFC
AF3_AFF5h	-42.25	70.44	22.16	Frontal_Mid_2_L	BA 9/46	DLPFC
AF3_AFz	-16.74	78.81	28.33	Frontal_Sup_2_L	BA 10	FPA
AF4_AFz	17.97	79.25	28.69	Frontal_Sup_2_R	BA 10	FPA
AF4_AFF6h	44.05	71.40	22.41	Frontal_Mid_2_R	BA 9/46	DLPFC
AF8_AFF6h	54.07	67.36	6.05	Frontal_Mid_2_R	BA 9/46	DLPFC
AF4_Fp2	32.79	81.31	7.44	Frontal_Sup_2_R	BA 10	FPA
F3_AFF5h	-50.52	58.58	32.64	Frontal_Mid_2_L	BA 9/46	DLPFC
F3_F1	-38.87	55.02	51.27	Frontal_Sup_2_L	BA 10	FPA
Fz_F1	-13.60	57.72	63.40	Frontal_Sup_2_L	BA 10	FPA
Fz_F2	14.91	58.05	63.00	Frontal_Sup_Medial_R	BA 9/10	mPFC
F4_F2	40.68	55.95	50.17	Frontal_Mid_2_R	BA 9/46	DLPFC
F4_AFF6h	52.12	59.68	31.84	Frontal_Mid_2_R	BA 9/46	DLPFC
FTT9h_T7	-84.14	-8.93	-19.57	Temporal_Mid_L	BA 21	MTG
TTP7h_T7	-84.86	-23.32	0.90	Temporal_Mid_L	BA 21	MTG
FTT9h_FT7	-82.45	6.13	-20.46	Temporal_Mid_L	BA 21	MTG
FTT7h_C5	-81.32	-6.46	18.87	Postcentral_L	BA 1/2/3	S1
TTP7h_C5	-82.92	-22.20	20.16	SupraMarginal_L	BA 40	SMG
FTT7h_T7	-83.26	-7.60	-0.38	Temporal_Mid_L	BA 21	MTG
FTT7h_FT7	-81.57	7.47	-1.28	Temporal_Sup_L	BA 22/41/42	STG